Available online at www.sciencedirect.com
SCIENCE DIRECT®
Journal of Chromatography A, 1003 (2003) 43–72
JOURNAL OF CHROMATOGRAPHY A
www.elsevier.com/locate/chroma

Repeatability and reproducibility of high concentration data in reversed-phase liquid chromatography I. Overloaded band profiles on Kromasil-C_{18}

Fabrice Gritti[a,b], Georges Guiochon[a,b,*]

[a]*Department of Chemistry, The University of Tennessee, 552 Buehler Hall, Knoxville, TN 37996-1600, USA*
[b]*Division of Chemical Sciences, Oak Ridge National Laboratory, Oak Ridge, TN, USA*

Received 17 January 2003; received in revised form 17 April 2003; accepted 17 April 2003

Abstract

Single-component adsorption-isotherm data were acquired by frontal analysis (FA) for six low-molecular-mass compounds (phenol, aniline, caffeine, theophylline, ethylbenzene and propranolol) on one Kromasil-C_{18} column, using water–methanol solutions (between 70:30 and 20:80, v/v) as the mobile phase. Propranolol data were also acquired using an acetate buffer (0.2 *M*) instead of water. The data were modeled for best agreement between calculated and experimental overloaded band profiles. The adsorption energy distribution was also derived and used for the selection of the best isotherm model. Widely different isotherm models were found to model best the data obtained for these compounds, convex upward (i.e. Langmuirian), convex downward (i.e. anti-Langmuirian), and S-shaped isotherms. Using the same sample size for all columns (loading factor, Lf≈10%), overloaded band profiles were recorded on four different columns packed with the same batch of Kromasil-C_{18} and five other columns packed with different batches of Kromasil-C_{18}. These experimental band profiles were compared to the profile calculated from the isotherm measured by FA on the first column. The repeatability as well as the column-to-column and the batch-to-batch reproducibilities of the band profiles are better than 4%.

Keywords: Adsorption isotherms; Band profiles; Frontal analysis; Mathematical modeling; Aniline; Caffeine; Phenol; Propranolol; Theophylline; Ethylbenzene

1. Introduction

The rapid development of the applications of preparative liquid chromatography in the pharmaceutical industry has led to the recent renewal of interest in the fundamentals of nonlinear chromatography [1,2]. It has now become possible to calculate the design and operating conditions of a separation that render optimum the value of any objective function, e.g. for maximum production rate, for minimum solvent consumption or for the optimum value of any combination of the production rate and the recovery yield [1,3]. However, this calculation requires a prior accurate understanding of the thermodynamics and the kinetics of the chromatographic process involved in the separation studied. The former is characterized by the competitive isotherms of the feed components, the latter by the

*Corresponding author. Tel.: +1-865-974-0733; fax: +1-865-974-2667.
E-mail address: guiochon@utk.edu (G. Guiochon).

0021-9673/03/$ – see front matter
doi:10.1016/S0021-9673(03)00685-X

rate coefficients of the various steps involved in mass transfer across the column [1,2].

It was demonstrated that thermodynamics controls band profiles, particularly at high concentrations and when the mass transfer kinetics is not very slow [1]. Accordingly, it determines, to a large extent, the recovery yield and the production rate that any industrial unit can achieve. For obvious economic reasons, preparative chromatography is carried out at high concentrations, the injected samples often being at concentrations close to those of the saturated solutions. Under such conditions, the equilibrium isotherms between the two phases of the chromatographic system are rarely linear. The stronger the nonlinear behavior of the isotherm at the maximum band concentration, the more unsymmetrical band profile, the lower the resolution of this band and its neighbors, hence the lower the recovery yield and the production rate [1,3]. Mass transfer kinetics affects the precise shape of the band profiles, dispersing to some extent the profiles predicted by thermodynamics alone. Accordingly, it may have a significant impact on the band resolution, especially at low column efficiencies [1].

It is thus of paramount importance to determine the competitive isotherms of the feed components. This task alone proves to be an important project for any laboratory. It may require several weeks for a pair of compounds. Fortunately, it has been shown that, in many instances, these competitive isotherms can be derived from the single-component isotherms of the compounds involved [1,4,5]. This latter task is far easier than the former.

Numerous methods are available for the acquisition of equilibrium isotherm data and for the derivation of single-component isotherms. The methods that are the fastest and the most convenient for this purpose are frontal analysis (FA) [1,5–7], elution by characteristic point (ECP) [1,8,9], pulse perturbations [1,10,11], and numerical inverse [12] methods. All of these methods have their own advantages and drawbacks which must be taken into account in any specific case in order to minimize measurement errors and costs [1]. In this work, we use the FA method, the most accurate but also the slowest and most costly.

The determination of single-component isotherms is thus essential to describe a chromatographic process. We know that adsorption phenomena are likely to be sensitive to several physico-chemical properties of the stationary phase. Variations in the column hydrophobic selectivity, methylene selectivity, silanol activity, or surface concentration of metal impurities have an impact on the retention factor of an analyte and also on the asymmetry of its peak and on the column efficiency. These properties vary significantly from column brand to column brand. Their reproducibility from batch to batch or even from column to column for columns packed with material of the same batch can be questioned. Recently, Kele and Guiochon studied under linear conditions the column-to-column and the batch-to-batch reproducibilities of four brands of packed RP-C_{18} columns [13–16] and those of a lot of monolithic columns [17]. As for columns packed with the Kromasil-C_{18} brand of RPLC packing materials, which will concern us in this paper, these authors showed that the column-to-column and batch-to-batch reproducibilities of the retention factors of 30 compounds of widely different chemical structures were typically between 0.2 and 1.3% and between 1 and 3%, respectively [14]. The relative standard deviations (RSDs) of the asymmetry factors of the neutral compounds of this set, measured on the columns packed with materials of different batches, were typically below 5%, values that were between two and 42 times higher than the RSD values measured for the repeatability of the results of these same measurements made on a single column. The batch-to-batch reproducibility of the efficiency of neutral compounds was characterized by RSDs below 10%. This high level of reproducibility measured at low concentrations of the analytes studied suggests that the reproducibility of the isotherm data measured at high solute concentrations may be similarly high. This issue is certainly worth exploring in some detail since the literature does not contain any systematic investigation of the batch-to-batch reproducibility of the performance of columns used in preparative chromatography.

The goal of this work was to determine the reproducibility of the adsorption isotherm data measured for different compounds, using different chromatographic systems, on a series of columns of the same brand, packed with particles of the same batch of bonded C_{18} silica or with particles of different

production batches. To save time and significant amounts of the solvent solutions and the sample compounds used in the FA experiments, the FA measurements were performed on one column only. These isotherm data were modeled and the best values of the model parameters were derived from a fit of the experimental data to the model. The isotherm so obtained was used to calculate the overloaded band profiles on the initial column and on nine other columns, four packed with the same batch of packing material, five others packed with material from different batches. The six compounds studied and seven mobile phase compositions used were selected so as to elicit as diverse isotherm profiles as possible, exhibiting from Langmuirian to anti-Langmuirian isotherm behavior. The degree of agreement between the calculated profile for each compound and the 10 experimental profiles obtained illustrates the column-to-column and batch-to-batch reproducibilities of the adsorption data that can be achieved with modern packing material in general and, more specifically, with Kromasil-C_{18} silica.

2. Theory

2.1. Determination of single-component isotherms by frontal analysis

Among the various chromatographic methods available to determine single-component isotherms, frontal analysis (FA) is the most accurate [1–4,6,7]. It consists in the step-wise replacement of the stream of mobile phase percolating through the column with streams of solutions of the studied compound of increasing concentrations and in the recording of the breakthrough curves at the column outlet. Mass conservation of the solute between the times when the new solution enters the column and when the plateau concentration is reached allows the calculation of the adsorbed amount, q^*, of the solute in the stationary phase at equilibrium at a given mobile phase concentration, C. This amount is best measured by integrating the breakthrough curve (equal area method) [18]. The adsorbed amount q^* is given by:

$$q^* = \frac{C(V_{eq} - V_0)}{V_a} \quad (1)$$

where V_{eq} and V_0 are the elution volume of the equivalent area and the hold-up volume, respectively, and V_a is the volume of stationary phase. This relationship applies to all breakthrough curves recorded. This method was used for the acquisition of all the experimental isotherm data measured in this work.

2.2. Models of single-component isotherm

All actual surfaces are heterogeneous. Such surfaces are usually studied as composites or quilts of homogeneous surfaces and are characterized by the distribution of the adsorption energies [19] or, in liquid–solid adsorption, by the distribution of adsorption affinities [20]. Accordingly, adsorption isotherms on homogeneous surfaces remain important. There are two such isotherms, those of Langmuir [1,5] and of Jovanovic [21].

2.2.1. The Langmuir Isotherm

The most popular isotherm for homogeneous surfaces is the Langmuir isotherm:

$$q = \frac{bq_s C}{1 + bC} \quad (2)$$

where b is the adsorption constant (see later) and q_s the saturation capacity. Since this model assumes that the surface studied is homogeneous, the adsorption affinity distribution is a Dirac δ-function. It defines one adsorption energy.

2.2.2. The Jovanovic isotherm

The Jovanovic isotherm is a modified version of the classical Langmuir isotherm [21]. The fundamental difference with the Langmuir isotherm is that this model considers the effect of collisions between the adsorbing and desorbing molecules on the desorption rate or number of desorbed molecules per unit time. This rate is then no longer proportional to the fraction of the surface covered by molecules. This assumption leads to the following new equation of the isotherm:

$$q^* = q_S[1 - \exp(-bC)] \quad (3)$$

This model cannot be mathematically reducible to a combination of local Langmuir isotherm. It defines itself a local adsorption isotherm.

2.2.3. The bi-Langmuir isotherm

This model is the simplest one that accounts for the adsorption behavior on a heterogeneous surface [22]. When this model applies, the surface can be considered as paved with two different types of homogeneous chemical domains which behave independently. Then, the equilibrium isotherm results from the addition of two independent local Langmuir isotherms:

$$q^* = q_{S,1} \cdot \frac{b_1 C}{1 + b_1 C} + q_{S,2} \cdot \frac{b_2 C}{1 + b_2 C} \quad (4)$$

As for the Langmuir isotherm, the equilibrium constants b_i are given by the following equation:

$$b_i = b_{0,i} e^{(\varepsilon_{a,i}/RT)} \quad (5)$$

where $\varepsilon_{a,i}$ is the adsorption energy on the sites i and $b_{0,i}$ is a preexponential factor that can be derived, in principle at least, from the molecular partition functions in the bulk and the adsorbed phases for the pure site i. In this model, there are two saturation capacities, $q_{S,1}$ and $q_{S,2}$, and two equilibrium constants, b_1 and b_2, each associated with an adsorption energy, $\varepsilon_{a,1}$ and $\varepsilon_{a,2}$, through Eq. (3). The energy distribution function is bimodal and both modes are represented by a Dirac δ-function [19].

2.2.4. The Toth isotherm

Toth proposed a semi-empirical isotherm model [23,24] to account for the experimental adsorption isotherms that are obtained on many heterogeneous adsorbents:

$$q^* = q_S \cdot \frac{bC}{[1 + (bC)^n]^{1/n}} \quad (6)$$

In this equation, q_S and b have the same meaning as in the Langmuir isotherm model and n is the heterogeneity parameter ($0 < n < 1$). This parameter increases with decreasing degree of surface heterogeneity. The distribution function is maximum for an adsorption energy equal to ε_a, the value of ε which is related to b through Eq. (3). This distribution is asymmetrical and unimodal, it tails toward the low adsorption energies [19].

2.2.5. The Ruthven isotherm

Simple considerations of statistical thermodynamics result in the following general adsorption isotherm equation [5]. In this model, the adsorbed molecules are localized in different surface sites or cages. Each cage contains a finite number of adsorbate molecules and may accommodate up to n of them. The model gives for single-component adsorption:

$$q^* = q_S \cdot \frac{C(a_1 + 2a_2 C + 3a_3 C^2 + \cdots + n a_n C^{n-1})}{1 + a_1 C + a_2 C^2 + 3a_3 C^3 + \cdots + a_n C^n} \quad (7)$$

where nq_S is the saturation capacity of the adsorbent and the coefficients a_i are related to the partition functions for an individual adsorbed molecule on the ith monomolecular layer. Assuming $n = 2$, Eq. (7) becomes that of the quadratic isotherm [1].

2.2.6. The extended liquid–solid BET model

The BET model of Brunauer, Emmett, and Teller is the most widely applied isotherm in gas–solid equilibrium. It assumes multilayer adsorption [25]. It was developed to describe adsorption phenomena in which successive molecular layers of adsorbate form at pressures well below the pressure required for the completion of the monolayer. The form of this model can be extended to liquid–solid chromatography. It was derived and discussed in detail elsewhere [26]. It has the following final expression:

$$q^* = q_S \cdot \frac{b_S C}{(1 - b_L C)(1 - b_L C + b_S C)} \quad (8)$$

where q_S is the monolayer saturation capacity of the adsorbent, b_S is the equilibrium constant for surface adsorption–desorption (over the free surface of the adsorbent) and b_L is the equilibrium constant for surface adsorption–desorption over a layer of adsorbate molecules. This model does not take surface heterogeneity into account and can be considered as a local adsorption isotherm.

2.3. Calculation of the adsorption energy distributions

Actual surfaces are not homogeneous, as was assumed so far and as is often assumed in analytical liquid–solid chromatography. Actual surfaces may be characterized by an adsorption energy distribution (AED). The experimental isotherm on such a surface is the sum of the isotherms on the different homogeneous fractions of the surface, fractions that correspond to a given energy of the AED. Under the condition of a continuous distribution, and assuming either a Langmuir or a BET local isotherm model, this sum can be replaced by an integral and the overall adsorption isotherm can then be written [15]:

$$q^*(C) = \int_0^\infty F(\varepsilon) \cdot \frac{b(\varepsilon)C}{1 + b(\varepsilon)C} \cdot \mathrm{d}\varepsilon \tag{9}$$

or

$$q^*(C) = \int_0^\infty F(\varepsilon) \cdot \frac{b(\varepsilon)C}{(1 - b_L C)(1 - b_L C + b(\varepsilon)C)} \cdot \mathrm{d}\varepsilon \tag{10}$$

for the Langmuir and for the BET local isotherms, respectively. The Langmuir local isotherm is used to describe the surface heterogeneity of strictly convex upward isotherms, while the BET local isotherm is more convenient for convex downward isotherms. In Eqs. (9) and (10), $q^*(C)$ is the total amount of solute adsorbed on the surface at equilibrium with a solution of concentration C, ε is the binding energy between an adsorbed solute molecule in the first layer and the surface of the adsorbent. b is the associated binding constant, equivalent to b_S in the case of the BET isotherm. b_L is a constant in the integral because it is assumed that the adsorption of the solute over a layer of solute is not influenced by the potential ε of the solid surface. The constant b can be expressed as:

$$b(\varepsilon) = b_0 \exp\left(\frac{\varepsilon}{RT}\right) \tag{11}$$

where b_0 is a preexponential factor that can be derived from the molecular partition functions in both the bulk and the adsorbed phases. The normalization condition for the AED is:

$$\int_0^\infty F(\varepsilon)\, \mathrm{d}\varepsilon = q_S \tag{12}$$

where q_S is the overall saturation capacity.

To characterize the behavior of a heterogeneous surface, the AED, $F(\varepsilon)$, is derived from the isotherm data, a procedure for which there is a wide variety of methods [19,27,28]. Most of them either use a preliminary smoothing of the experimental data and fit them to an isotherm model, or they search for an AED given by a certain function. In this work, we used the EM method [27,29]. This is a computer-intensive method that uses directly the raw experimental data without injecting any arbitrary information in the derivation. The distribution function $F(\varepsilon)$ is discretized using N-grid points in the energy space (i.e. assuming that the surface is made of a set of N homogeneous surfaces) and the corresponding values of $F(\varepsilon)$ are estimated from the data points. The energy space is limited by ε_{min} and ε_{max}. These values are obtained from the maximum and minimum concentrations applied in FA [27,29] by using Eq. (10) ($b_{min} = 1/C_{max}$, $b_{max} = 1/C_{min}$) but other intervals may be considered as long as they include the data. The amount $q(C_i)$ of solute adsorbed at concentration C_j is iteratively estimated by calculating (for $j = 1, \ldots, M$; $i = 1, \ldots, N$):

$$q^k_{cal}(C_j) = \sum_{\varepsilon_{min}}^{\varepsilon_{max}} F^k(\varepsilon_i) \cdot \frac{b(\varepsilon_i)C_j}{1 + b(\varepsilon_i)C_j} \cdot \Delta\varepsilon \tag{13}$$

for a local Langmuir isotherm model or

$$q^k_{cal}(C_j) = \sum_{\varepsilon_{min}}^{\varepsilon_{max}} F^k(\varepsilon_i) \cdot \frac{b(\varepsilon_i)C_j}{(1 - b_L C_j)(1 - b_L C_j + b(\varepsilon_i)C_j)} \cdot \Delta\varepsilon \tag{14}$$

for a BET local isotherm, with, in both cases:

$$\Delta\varepsilon = \frac{\varepsilon_{max} - \varepsilon_{min}}{N - 1} \quad \varepsilon_i = \varepsilon_{min} + (i - 1)\,\Delta\varepsilon \tag{15}$$

The index k indicates the kth iteration of the numerical calculation of the AED function. For the initial guess (iteration $k = 0$) of the AED function, we take for $F(\varepsilon_i)$ the uniform distribution over the N fictitious adsorption sites of the maximum adsorbed

amount observed experimentally. This initial guess has the advantage of introducing the minimum possible bias into the AED calculation:

$$F^0(\varepsilon_i) = \frac{q(C_M)}{N} \quad \forall i \in [1, N] \tag{16}$$

While the local Langmuir and Jovanovic models of local adsorption depend only on the binding constant between the solute and the local surface, the BET isotherm includes another constant, b_L, which measures the interaction energy between layers. Its value must be chosen arbitrarily. A valid choice of b_L should lead to an overall saturation capacity q_S that makes physical sense and to a good agreement between the calculated and experimental isotherms.

Actually, the EM program calculates the amount adsorbed by taking $b(\varepsilon_i)$ as the variable in the energy space, so that neither the temperature nor the pre-exponential factor need to be defined. Only M, N, b_{min}, b_{max} and the number of iterations must be specified at the beginning of the calculation. b_{min} and b_{max} are related to the reciprocal of the highest and the lowest concentration applied in FA, respectively. It is noteworthy that, to obtain any information on the adsorption energy, an assumption must be made for b_0 in Eq. (10). The final result is the distribution of the equilibrium constants.

The distribution function is updated after each iteration by:

$$F^{k+1}(\varepsilon_i) = F^k(\varepsilon_i) \sum_{c_{min}}^{c_{max}} \frac{b(\varepsilon_i)C}{1 + b(\varepsilon_i)C} \cdot \Delta\varepsilon \cdot \frac{q_{exp}(C_j)}{q^k_{cal}(C_j)} \tag{17}$$

and

$$F^{k+1}(\varepsilon_i) = F^k(\varepsilon_i) \sum_{c_{min}}^{c_{max}} \frac{b(\varepsilon_i)C_j}{(1 + b_L C_j)(1 - b_L C_j + b(\varepsilon_i)C_j)} \cdot \Delta\varepsilon \cdot \frac{q_{exp}(C_j)}{q^k_{cal}(C_j)} \tag{18}$$

for the Langmuir and BET local isotherms, respectively.

The EM procedure protects better than most other methods against the consequences of the possible incorporation of experimental artifacts into the calculation of AED or against the effect of modeling the experimental data.

2.4. Modeling of high-performance liquid chromatography

The profiles of overloaded bands were calculated using the equilibrium-dispersive (ED) model of chromatography [1,5,30]. This model assumes instantaneous equilibrium between the mobile and the stationary phases and a finite column efficiency. The latter is assumed to originate from an apparent axial dispersion coefficient, D_a, accounting for all the dispersive phenomena (molecular and eddy diffusion and non-equilibrium effects) that take place in a chromatographic column. The axial dispersion coefficient is:

$$D_a = \frac{uL}{2N} \tag{19}$$

where u is the mobile phase linear velocity, L the column length, and N the number of theoretical plates or apparent efficiency of the column.

In this model, the mass balance equation for a single component is stated in the following equation [1]:

$$\frac{\partial C}{\partial t} + u \cdot \frac{\partial C}{\partial z} + F \cdot \frac{\partial q^*}{\partial t} - D_a \cdot \frac{\partial^2 C}{\partial z^2} = 0 \tag{20}$$

where q^* and C are the stationary and mobile phase concentrations of the adsorbate, respectively, t is the time, z the distance along the column, $F = (1 - \varepsilon)/\varepsilon$ is the phase ratio, and ε is the total column porosity, a function of the local concentration [26]. q^* is related to C through the isotherm equation, $q^* = f(C)$.

2.4.1. Initial and boundary conditions for ED model

At $t = 0$ the concentration of the adsorbate in the column is uniformly equal to zero and the stationary phase is in equilibrium with the pure mobile phase. The boundary conditions used are the classical Dankwerts-type boundary conditions [31] at the inlet and outlet of the column.

2.4.2. Numerical solutions of the ED model

The ED model was solved using the Rouchon program based on the finite difference method [1,32–34].

3. Experimental

3.1. Chemicals

The mobile phase used in this work, whether for the determination of the adsorption isotherms data or for the recording of large size band profiles, was a mixture of HPLC-grade methanol and water (30:70, v/v, for caffeine and theophylline; 40:60, v/v, for propranolol without buffer; 45:55, v/v, for phenol and aniline; 60:40, v/v, for propranolol with an acetate buffer at 0.2 *M* and pH 5.9; and 80:20, v/v for ethylbenzene), both purchased from Fisher Scientific (Fair Lawn, NJ, USA). The solvents used to prepare the mobile phase were filtered before use on an SFCA filter membrane, 0.2 μm pore size (Suwannee, GA, USA). Uracil, aniline, caffeine, theophylline, phenol, propranolol, ethylbenzene, acetic acid and sodium acetate were obtained from Aldrich (Milwaukee, WI, USA).

3.2. Materials

Ten manufacturer-packed Kromasil-C_{18}, 250×4.6 mm, columns were used (column serial numbers E6019, E6021–E6024, E6103–E6106 and E6436, all from Eka Nobel, Bohus, Sweden). For the sake of simplicity, they will be referred to as columns I to X (corresponding to Table 1). These C_{18}-silica bonded, endcapped, packed columns were previously used by Kele and Guiochon [14] in their study of the reproducibility of the properties of RPLC columns under linear conditions. The main characteristics of the bare silica and of the packing material used for these columns are summarized in Table 1.

The hold-up time of each column was determined from the retention time of two consecutive injections of uracil carried out immediately before that of each compound injected. For mobile phase compositions in the range 30:70 to 80:20 (v/v), the elution time of uracil is nearly the same as that of methanol or sodium nitrate. Its measurement permits the determination of an excellent estimate of the column void volume that is necessary for the band profile calculations. The values measured for the total porosity ε of the 10 columns used in this work are listed in Table 2.

3.3. Apparatus

The data were acquired using a Hewlett-Packard (now Agilent Technologies, Palo Alto, CA, USA) HP 1090 liquid chromatograph. This instrument includes a multi-solvent delivery system (tank volume, 1 dm^3 each), an auto-sampler with a 25-μl loop, a diode-array UV-detector, a column thermostat and a computer data acquisition station. Compressed nitrogen and helium bottles (National Welders, Charlotte, NC,

Table 1
Physico-chemical properties of the 10 packed Kromasil-C_{18} columns (Eka)

Column	Bare silica batch					Silica-C_{18} batch	
	Particle size (μm)	Particle size distribution (90:10, % ratio)	Pore size (Å)	Surface area (m^2/g)	Na, Al, Fe content (ppm)	Total carbon (mass %)	Surface coverage ($mmol/m^2$)
E6019 (I)	5.98	1.44	112	314	11; <10; <10	20.00	3.59
E6021 (II)	5.98	1.44	112	314	11; <10; <10	20.00	3.59
E6022 (III)	5.98	1.44	112	314	11; <10; <10	20.00	3.59
E6023 (IV)	5.98	1.44	112	314	11; <10; <10	20.00	3.59
E6024 (V)	5.98	1.44	112	314	11; <10; <10	20.00	3.59
E6103 (VI)	5.98	1.44	112	314	11; <10; <10	19.65	3.51
E6104 (VII)	5.98	1.44	112	314	11; <10; <10	19.85	3.55
E6105 (VIII)	6.03	1.38	112	322	15; <10; <10	20.00	3.50
E6106 (IX)	6.24	1.48	107	333	23; <10; <10	20.60	3.52
E6436 (X)	6.11	1.46	114	313	15; 13; 14	19.80	3.55

Table 2
Total porosities of the 10 packed Kromasil-C_{18} columns (Eka) measured by the injection time of uracil at a flow rate of 1 ml/min for the seven compounds studied. The extra-column volume was 0.068 ml. The volume of the column tubes is 4.155 ml

Column	Mobile phase (methanol–water, v/v)						
	30:70		40:60, Propranolol (no buffer)	45:55		60:40, Propranolol (with buffer acetate)	80:20, Ethylbenzene
	Caffeine	Theophylline		Phenol	Aniline		
E6019 (I)	0.6325	0.6359	0.6044	0.5919	0.5945	0.5760	0.5712
E6021 (II)	0.6407	0.6404	0.6061	0.5962	0.5955	0.5774	0.5724
E6022 (III)	0.6395	0.6370	0.6039	0.5919	0.5935	0.5760	0.5707
E6023 (IV)	0.6376	0.6372	0.6037	0.5930	0.5940	0.5772	0.5688
E6024 (V)	0.6345	0.6324	0.6024	0.5882	0.5882	0.5760	0.5683
E6103 (VI)	0.6376	0.6364	0.6039	0.5952	0.5926	0.5767	0.5692
E6104 (VII)	0.6402	0.6419	0.6070	0.5964	0.5960	0.5793	0.5721
E6105 (VIII)	0.6453	0.6438	0.6106	0.6015	0.5988	0.5846	0.5762
E6106 (IX)	0.6347	0.6318	0.5967	0.5866	0.5858	0.5700	0.5618
E6436 (X)	0.6128	0.6120	0.5805	0.5719	0.5690	0.5550	0.5471

USA) are connected to the instrument to allow the continuous operation of the pump and auto-sampler. The extra-column volumes measured from the auto-sampler and the pump system to the column inlet are 0.068 and 0.90 ml, respectively. All the retention data were corrected for this contribution. The flow-rate accuracy was controlled at 23 °C by pumping at 1 ml/min during 50 min the pure mobile phase from each of the pump heads to a volumetric glass of 50 ml. A relative error of less than 0.4% was observed, so we can estimate the accuracy of the flow-rate at 4 ml/min at flow rates around 1 ml/min. All measurements were carried out at a constant temperature of 23°C, fixed by the laboratory temperature controller. From the morning to the evening of any day, the variation in temperature never exceeded 1 °C.

3.4. Frontal analysis isotherm measurements on column I

The mobile phase composition at which the FA measurements were performed on the reference column (E6019 or column I) depended on the retention factor at infinite dilution of the solute considered. In order to acquire a sufficient number of data points and to achieve accurate measurements, the retention factor should be neither too high (which would be time-consuming) nor too low (which would cause a decrease in accuracy). Values of k' between 2 and 3 are ideal. Prior to any isotherm determination, the solubilities at 23 °C of all the compounds in their respective mobile phase were determined approximately by the stepwise addition of 0.5 ml of the pure mobile phase into a volume of 25 ml of a saturated solution containing a small amount of undissolved compound until its complete dissolution. Accordingly, the maximum concentrations (in the corresponding mobile phase) used in the FA measurements were 30, 64, 34, 9.5, 40, 44 and 40 g/l for phenol, aniline, caffeine, theophylline, propranolol (without buffer), ethylbenzene and propranolol (with acetate buffer), respectively. Two master sample solutions were prepared, with concentrations of 15% and 100% of these maximum concentrations, respectively. Two consecutive series of FA measurements were carried out with these two solutions (see procedure below), covering a wide range of concentrations. Thirty-two experimental adsorption data points were recorded for each compound.

One pump of the HPLC instrument was used to deliver a stream of the pure mobile phase, the second pump a stream of pure sample solution. The concentration of the studied compound is determined by the concentration of the mother sample solution and by the ratio of the flow rates delivered by the two pumps. The breakthrough curves are recorded successively at a flow rate of 1 ml/min, with a

sufficiently long time interval between each breakthrough curve to allow for the reequilibration of the column with the pure mobile phase. The injection time of each new solution was 5 min, which was sufficient in order to reach a stable plateau at the column outlet.

The overloaded profiles (a total of nine band profiles) needed for the validation of the fitted isotherms (column I) were recorded at the time when the frontal analysis experiments were carried out. The band profile corresponding to the highest loading factor (Lf around 10%) will be compared to those recorded with the other nine columns.

3.5. Measurements of overloaded profiles on columns II to X

A reserve of 4 l of the mobile phase (a mixture of methanol and water at various compositions, depending on the sample, see earlier) was prepared before performing FA measurements on column I. The mixing of methanol and water is exothermic and it takes at least 5 h for its temperature to stabilize at room temperature (23 °C). This amount of mobile phase was used, first, for the measurements of the adsorption isotherm data on column I, then for the recording of the overloaded profiles on this column, and finally for the recording of four overloaded profiles on each one of columns II to X. Using the same mobile phase with each column was of paramount importance in order to reduce the unavoidable experimenter errors when a mobile phase mixture is manually prepared. The columns I to X were used in the same order for the study of all compounds.

For each column II to X, the following sequence was followed. Firstly, the column was equilibrated with the pure mobile phase for at least 120 min. If after this time the UV detector signal was still drifting or had a background noise of more than 0.2 mAU, an additional equilibration time of 30 min was applied until full equilibration was considered to have been reached. Secondly, the column dead volume and the sample retention time at infinite dilution were measured by performing two successive 2-μl injections of a uracil and a sample solution, both at concentrations of about 1 g/l of the respective compound in the corresponding mobile phase. It was observed that the total porosity of each column decreases steadily with decreasing water content of the mobile phase (Table 2), by ~10% when the composition varies from 30:70 (v/v) to 80:20 (v/v) methanol–water. Finally, four overloaded profiles, with samples of increasing sizes, were recorded. For the sake of clarity, only one of them will be presented later in this work, the one corresponding to the highest loading factor (around 10%). It corresponds to the injection for 54 s of a sample solution at a concentration of 90% of the one used in the FA measurements made with column I.

3.6. Comparison between calculated and experimental band profiles

3.6.1. Parameters used to calculate the band profiles

In this work, the calculations of all band profiles were done by using the equilibrium dispersive model of chromatography and the Rouchon–Golshan numerical method [1,32–34]. The input parameters needed to run these calculations are: the mobile phase flow rate, the column length, the column total porosity, its number of theoretical plates, the inlet concentration profile (or boundary condition at column inlet) and the isotherm parameters.

The flow rate was set at 1 ml/min for all measurements. The length of all the columns is 25 cm. Their total porosities are tabulated in Table 2, for all the columns and mobile phase compositions. The total porosity does not need to be a constant parameter in the calculations because the concentration of the sample in the adsorbed phase does not depend on the column void volume nor on the time spent by the solute in the mobile phase. Adsorption and the retention factor depend on the chemical nature of the bare silica (mesopore structure, number and strength of the active sites, metal impurities . . .) and on the modifications of the surface chemistry resulting from the C_{18} bonding (carbon content, C_{18} chain density). Those are all surface properties. Then, all the band profiles are calculated according to the measured values of the column total porosity (Table 2). By contrast, the number of theoretical plates N of the columns was kept constant for all columns. Surface properties may influence the mass transfer kinetics, hence the overall column efficiency, however, the

effect on band profiles under the conditions of this study is modest [1]. The common efficiency was derived from the results of the calculations performed on the reference column. The efficiency was chosen in order to minimize the differences between the calculated and experimental shape of the concentration shock layers propagating under constant pattern conditions [1,26]. Fig. 1 illustrates how the best efficiency was chosen for column I. Finally, the actual inlet profile of the injection made with Lf = 10% had been measured before the beginning of the FA measurements. It was fitted to a combination of two Gaussian functions separated by a delay. This realistic injection profile was used as the inlet boundary conditions for the whole series of calculations instead of the classical approximation by a rectangular inlet profile.

The isotherm parameters used in all calculations were those derived from the FA measurements made on the reference column I. The best isotherm model was selected after the following procedure. First the data were fitted to all the models of isotherms discussed in Section 2, using a nonlinear regression, and their Fisher number, that qualifies the quality of fit [1,2], were calculated. Those models whose Fisher numbers were below 10 000 were dismissed. Secondly, band profiles were calculated using the remaining isotherms and the model which gave overloaded profiles in best agreement with the experimental ones was kept. If two models describe equally well the experimental overloaded profiles, their affinity energy distributions were derived from the raw adsorption data, using the procedure elaborated by Stanley et al. [27], and these AEDs were compared to the theoretical AED function of the two models. Application of this method for the discrimination of isotherm models was described previously [35]. The best isotherm finally selected was used for all further calculations.

3.6.2. Definitions

As will become apparent later, the shape of the calculated overloaded band profiles agree excellently with those of the experimental profiles. For a loading factor close to 10%, the same efficiency ($N \approx 2500$) describes well the band profiles of all the compounds studied, on all the columns used. Actually, this

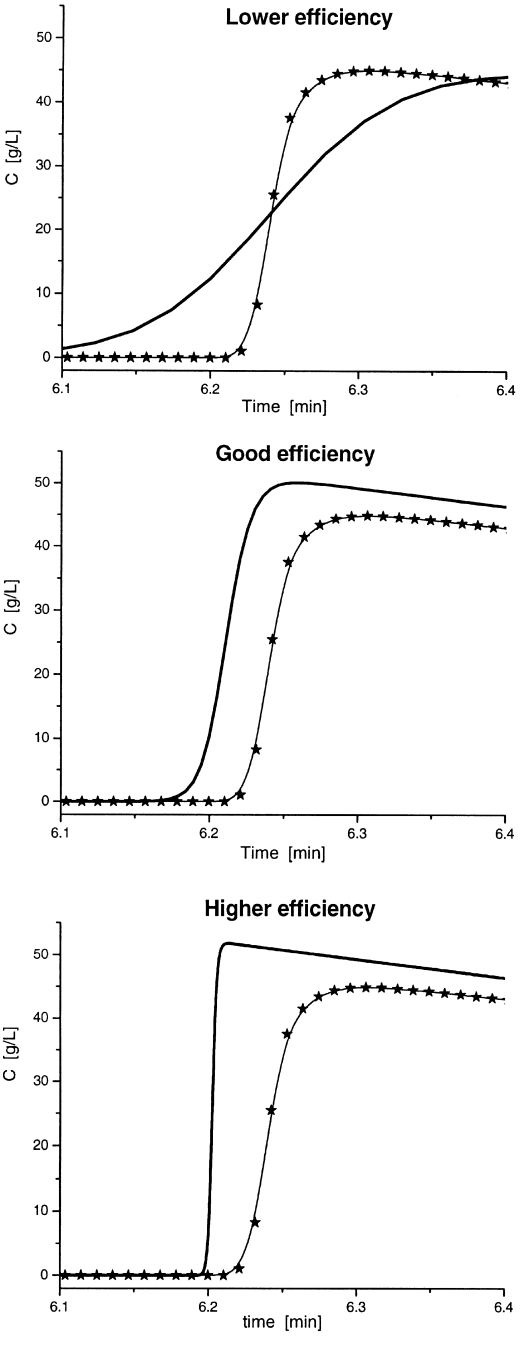

Fig. 1. Determination of the best column efficiency used to perform the calculation of band profiles with all the columns. Analysis of the shock layer profile propagating under constant pattern condition. The best value of the efficiency gives a calculated profile that has the same slope for the shock $\Delta q/\Delta C$ as the experimental profile.

means that, provided we use a constant dispersive correction, the presence and the locations of all the diffuse and self-sharpening fronts observed in all the experimental bands are well accounted for by an adsorption behavior following the one described by the selected isotherm models. The only significant changes observed between the calculated and the experimental profiles were small shifts in the time positions of these fronts. These changes are due to small numerical differences in the values of the isotherm parameters. They characterize the reproducibility of the packing material studied.

In this work, we focus our attention on the relative positions of the shock layers and the diffuse fronts in the calculated and experimental profiles. Three main families of overloaded peak profiles were encountered. Each one corresponds to a group of isotherm models. Three main families of isotherms can be described.

1. The convex upward isotherms also called Langmuirian. The profiles exhibit a front shock layer and a diffuse rear (Fig. 2A). This isotherm family includes the Langmuir, the Jovanovic, the bi-Langmuir, and the Toth isotherm models. One of these models accounts best for the adsorption behavior of aniline, caffeine, phenol, theophylline and propranolol when the mobile phase was made with an aqueous acetate buffer.
2. The S-shaped type isotherms of the first kind. These isotherms are convex downward at low concentrations, convex upward at high concentrations. Accordingly, a high concentration band profile exhibits a diffuse front at low concentrations and a shock front at high concentrations followed with a diffuse rear at high concentrations and a shock rear at low concentrations (Fig. 2C). When the mobile phase is unbuffered, propranolol gave bands with this profile shape and the quadratic isotherm was best for this compound.
3. The S-shaped isotherms of the second kind. These isotherms are convex upward at low concentrations, convex downward at high concentrations. Accordingly, a high concentration band profile exhibits a shock front layer at low concentrations and a diffuse front at high concentrations followed with a rear shock at high concentrations and a diffuse rear at low concentrations (Fig. 2B).

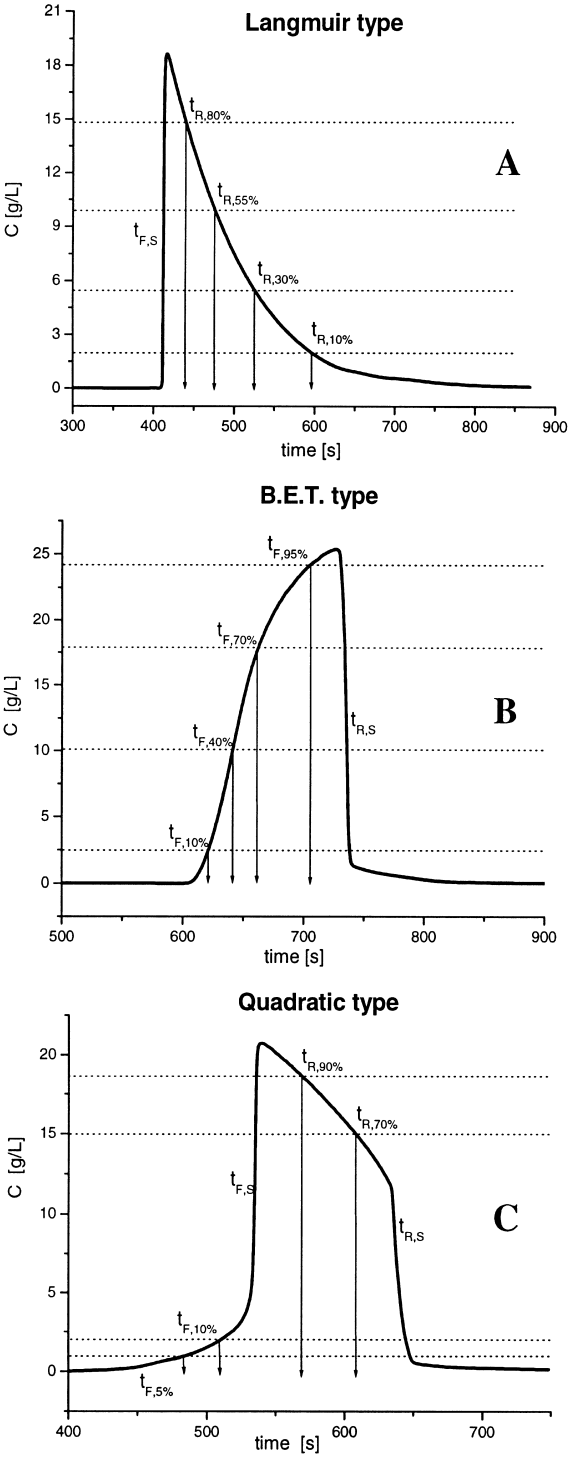

Fig. 2. Arbitrary choice for a discretization of the band profile. (A) Jovanovic, Toth and bi-Langmuir isotherms. (B) BET isotherm. (C) Quadratic isotherm.

Ethylbenzene gave bands with this shape and the BET model was the best for this compound.

3.6.3. Comparison between band profiles

In order to compare the calculated and the experimental overloaded profiles, we defined a number of characteristic points of the profile curves (see Fig. 2). Then we determined the column-to-column variations of the profiles by a combination of the changes in position of the points. In the case of the first profile type (Fig. 2A), we defined five points. The first point is defined by the retention time of the shock front and the four others are the times on the rear diffuse profile when the concentration of the band is equal to 80%, 55%, 30% and 10% of the maximum band concentration. In the case of Fig. 2B, we defined the retention times of the rear shock and of the times when the concentration on the diffuse front of the band is equal to 10%, 40%, 70% and 95% of the maximum band concentration. In the last case (Fig. 2C), we defined six times as the retention times of the front and the rear shocks and the times when the concentration on the diffuse front is equal to 5% and 10% of the maximum concentration and when the concentration on the rear diffuse front is equal to 90% and 70% of the maximum concentration of the band.

For a given column, the relative difference between calculated and experimental profiles is calculated as:

$$E(C) = \frac{1}{N} \cdot \sum_i a_i \cdot \frac{t_i^{\mathrm{Calc}} - t_i^{\mathrm{Exp}}}{t_i^{\mathrm{Exp}}} \quad (21)$$

where N is the number of points compared in the experimental and calculated profiles, i is the rank of the points, a_i is a weight given to the point i, t is the time measured on the experimental profile and t is the corresponding value on the calculated profile. This definition of the difference between the two profiles is arbitrary. The value of E can be positive or negative, depending on whether the calculated profile elutes mostly before or after the experimental one. E depends on the arbitrary selection of the points chosen to describe as best as possible the whole overloaded profile with the fewest number of points. It has no fundamental meaning but is a useful tool to compare simply the behavior of the different columns. Because shocks are more important parts of the profiles than diffuse boundaries, they are given a heavier weight. The front and rear parts of the profile should count equally. So, in the first case, the front being a pure shock, the weight of the corresponding point is four, equal to the sum of the weights of the four points chosen to describe the rear diffuse boundary. In the second case (Fig. 2B), this is the same situation and the weights of the points at the shock and on the diffuse front boundary are four and one, respectively. In the last case (Fig. 2C), there are two shocks and four points on diffuse boundaries. So the weights of the two shock points are two and those of the four points on the continuous boundaries are unity.

4. Results and discussion

4.1. Measurement of the hold-up volumes and retention factors on the 10 columns

4.1.1. Reproducibility of the dead volumes measured on the 10 columns

Fig. 3 illustrates the column-to-column reproducibility of the column hold-up volume on the 10 Kromasil columns and its dependence on the nature of the chromatographic system selected (mobile phase composition). The RSD of the hold-up volume of the five columns packed with the same batch of packing material (columns I to V) varies between 0.1% and 0.5%. By contrast, the RSD estimated for the six columns packed with different batches of the material (columns I and VI to X) is constant for all the chromatographic systems, at 1.8%. The data in Fig. 3A suggest that the column-to-column fluctuations of the hold-up volumes depend on the nature of the silica material used to bind the C_{18} alkyl chains (see the different results for columns VIII, IX and X on the one hand, for columns VI and VII on the other hand). Note that the particle porosity increases with increasing methanol concentration in the mobile phase. When this concentration increases from 30% to 80% the decrease in porosity is uniform over all the 10 columns, at ~0.28 cm^3 (Fig. 3B). This suggests that the amount of C_{18} chains bonded to the different silica batches is nearly the same for all the Kromasil-C_{18} batches.

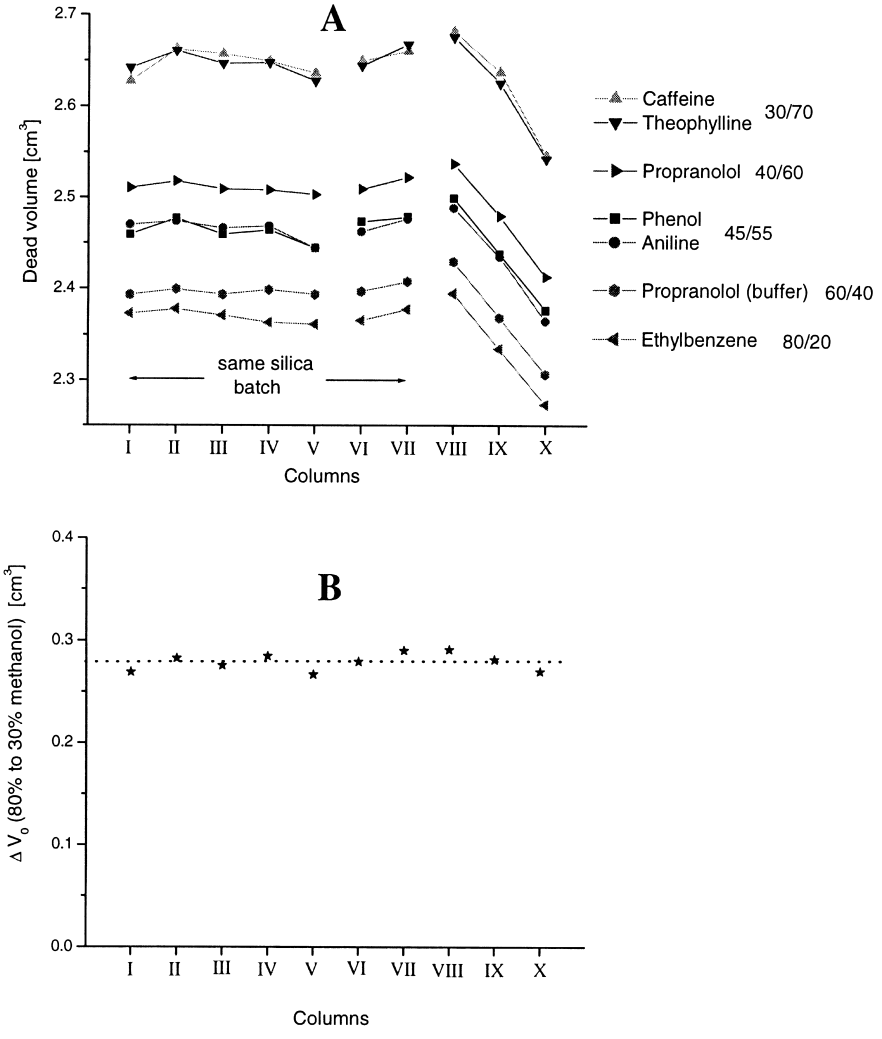

Fig. 3. (A) Hold-up volumes of the 10 columns for the different chromatographic systems used in this study. (B) Decrease of the total hold-up volume of the 10 columns when the methanol content of the mobile phase increases from 30% to 80% in volume. Note the uniformity of this decrease over all the columns.

4.1.2. Reproducibility of the retention factors measured on the 10 columns: comparison with 4-year-old data

Fig. 4 illustrates the column-to-column reproducibility of the retention factors at infinite dilution of the six compounds studied on the 10 Kromasil columns. This measurement was not possible for propranolol because, in the absence of buffer, the positively charged, acidic form of propranolol is unstable at infinite dilution when the pH is imposed by the mobile phase. At very low concentrations, this weak acid becomes strong and its dissociation is complete. So, it was impossible to detect clearly the elution of the ammonium form of propranolol and to measure its retention factor.

The column-to-column RSD of the retention factors within a batch (i.e. for the five columns packed with the same batch, columns I to V) varies between 0.3% and 1.4%. The batch-to-batch RSD (i.e. for the six columns packed with different batches) varies between 2.5% and 4.3%. These values are similar to those found 4 years ago on the same columns, with

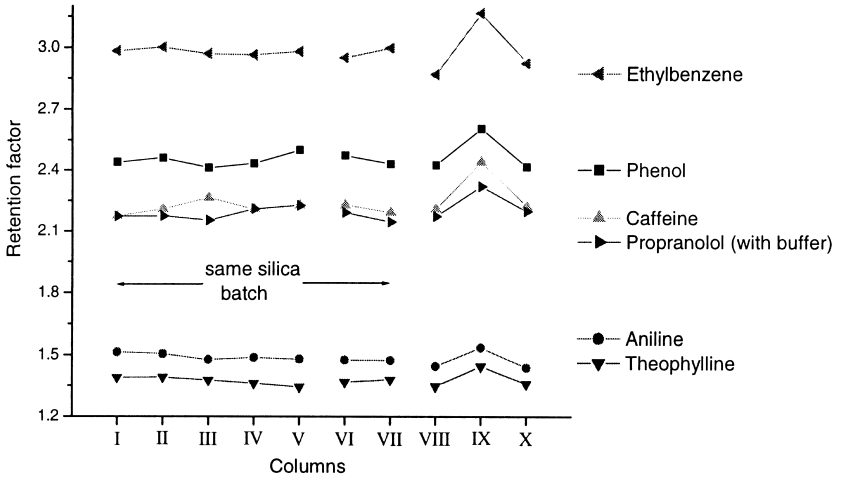

Fig. 4. Retention factor k' of the six solutes measured on the 10 columns. Note the systematic higher retention factor measured on column IX.

the same solutes, but similar mobile phase compositions by Kele and Guiochon [14]. It is noteworthy that one column give results that are significantly different from the other ones. Column IX gives the highest retention factor for all the solutes. This column is easily noticed in the earlier paper [14] where a figure equivalent to Fig. 4 was shown. We note that this column has the highest total mass of carbon (20.60% instead of 20% or less for all the other columns, see Table 1) but column VI with the lowest carbon mass gives the same results as the other column.

To summarize, the results obtained in linear conditions are in full agreement with those already found 4 years before with the same chromatographic systems. In spite of their long storage under pure acetonitrile, these columns are still effective and are reasonably representative of the production of the manufacturer. The results of their investigation under non-linear conditions should inform on the reproducibility to be expected from the packing materials used for preparative RPLC.

4.2. Measurement of adsorption isotherms on the reference column I

The reference column (column I) was chosen arbitrarily among the five columns packed with packing material of the same batch, in order to measure the adsorption data by FA. Five different chromatographic conditions were selected in order to measure the adsorption isotherm data of aniline, phenol, caffeine, theophylline and ethylbenzene. In addition, the adsorption data of propranolol were measured with two mobile phases, one made with neat water, the other with an aqueous buffer. In the next sections, we briefly describe the results of these measurements and of the modeling of data for these seven chromatographic systems. For each system, we present the isotherm data (symbols) and the best model (line), the best affinity distribution energy function, and a comparison between one experimental overloaded band profile (Loading factor≈10%) and the corresponding calculated profile. Table 3 summarizes the numerical values of the isotherm parameters and the Fisher parameters.

4.2.1. Adsorption of aniline (45:55, v/v): Jovanovic isotherm

The best model accounting for the adsorption data of aniline is the Jovanovic isotherm (Fig. 5). The Langmuir isotherm fails because of a lower Fisher number (12 000 versus 30 000 for the Jovanovic isotherm) and a much too high value of the saturation capacity (about 400 g/l), which has no clear physical sense. Fig. 5A shows the best fit obtained for the data and the good agreement between the experimental and calculated overloaded band pro-

Table 3
Adsorption isotherm fitting of the seven adsorption systems on the Kromasil-C_{18} column I. Fisher test values and best isotherm parameters obtained by regression analysis on five different models of isotherm (bi-Langmuir, BET, second-order Ruthven or quadratic, Jovanovic and Toth isotherms)

Bi-Langmuir	Fisher	$q_{s,1}$ (g/l)	b_1 (l/g)	$q_{s,2}$ (g/l)	b_2 (l/g)
Caffeine	133 900	171.2	0.01612	6.54	0.19030
Phenol	118 600	128.3	0.00993	38.7	0.06338
Propranolol	41 600	152.72	0.00975	7.64	0.19054

BET	Fisher	q_s (g/l)	b_S (l/g)	b_L (l/g)
Ethylbenzene	51 200	167.0	0.02566	0.01090

Quadratic	Fisher	q_S (g/l)	a_1 (l/g)	a_2 (l^2/g^2)
Propranolol	22 230	90.4	0.03005	0.00129

Toth	Fisher	q_S (g/l)	b (l/g)	n
Theophylline	64 500	186.8	0.01367	0.8526

Jovanovic	Fisher	q_S (g/l)	b (l/g)
Aniline	31 430	183.5	0.01290

files. The AED is unimodal (adsorption constant of 0.0129 l/g), with an overall saturation capacity of 183.5 g/l when a local Jovanovic isotherm is assumed.

4.2.2. Adsorption of theophylline (30:70, v/v): Toth isotherm

The best isotherms for the adsorption data of theophylline were either the Toth or the bi-Langmuir model. Because the AED obtained was unimodal, the Toth isotherm was definitely the best model (Fig. 6). The best values of the saturation capacity, adsorption constant and the heterogeneity parameter were 187 g/l, 0.01367 l/g and 0.853, respectively. This last value suggests a relatively important heterogeneity of the surface, contrasting with the result obtained of a homogeneous surface for the basic aniline.

4.2.3. Adsorption of phenol (45:55, v/v), caffeine (30:70, v/v) and propranolol (60:40, v/v with buffer): bi-Langmuir isotherm

For these three compounds, the bi-Langmuir isotherm model was the model that accounts best for the adsorption data (Figs. 7–9). The selection of the bi-Langmuir model is well supported by high values of the Fisher coefficient and by the finding in all cases of a bi-modal AED function estimated from the raw adsorption data [35]. The high energy sites have a much higher collective saturation capacity for phenol (Fig. 7) than for propranolol and caffeine (Figs. 8 and 9, and Table 3). The best isotherm parameters are listed in Table 3. Note the similarity between the high energy site adsorption constants for propranolol and caffeine.

4.2.4. Adsorption of ethylbenzene (80:20, v/v): BET isotherm

The adsorption isotherm of ethylbenzene is convex downward at high concentrations (Fig. 10). The best model accounting for the FA experiments is the extended liquid–solid BET model previously described [26]. The energy distribution is unimodal if the calculation is performed assuming a local BET isotherm model [36].

4.2.5. Adsorption of propranolol (40:60, v/v, with no buffer): quadratic isotherm

In the absence of a buffer in the mobile phase, the adsorption isotherm of propranolol is no longer convex upward. It does not follow bi-Langmuir but S-shape isotherm behavior. It is an anti-Langmuir isotherm at low concentrations, then becomes convex upward at high concentrations. The FA adsorption data fitted very well to several isotherm models such

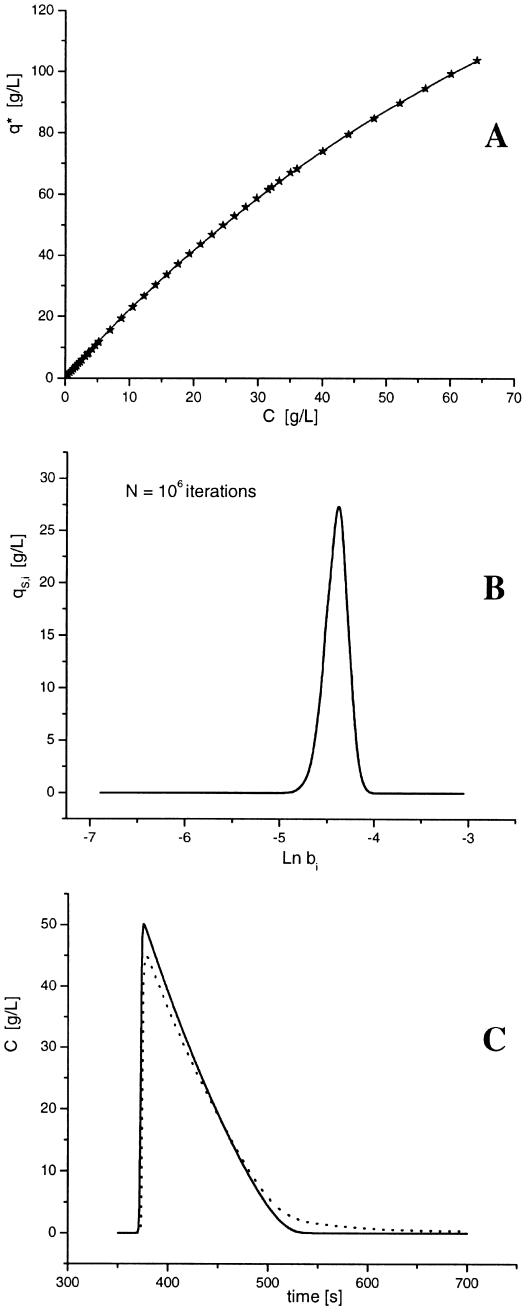

Fig. 5. (A) Experimental isotherm (stars) and best Jovanovic isotherm (solid line) of aniline on the packed Kromasil-C_{18} column I with methanol–water (45:55, v/v) as the mobile phase. $T = 295$ K. (B) Unimodal adsorption energy distribution calculated from the raw adsorption data by the expectation-maximization method. Local Langmuir isotherm. (C) Comparison between calculated (solid line) and experimental band profile (dashed line) measured on column I, Lf = 10%.

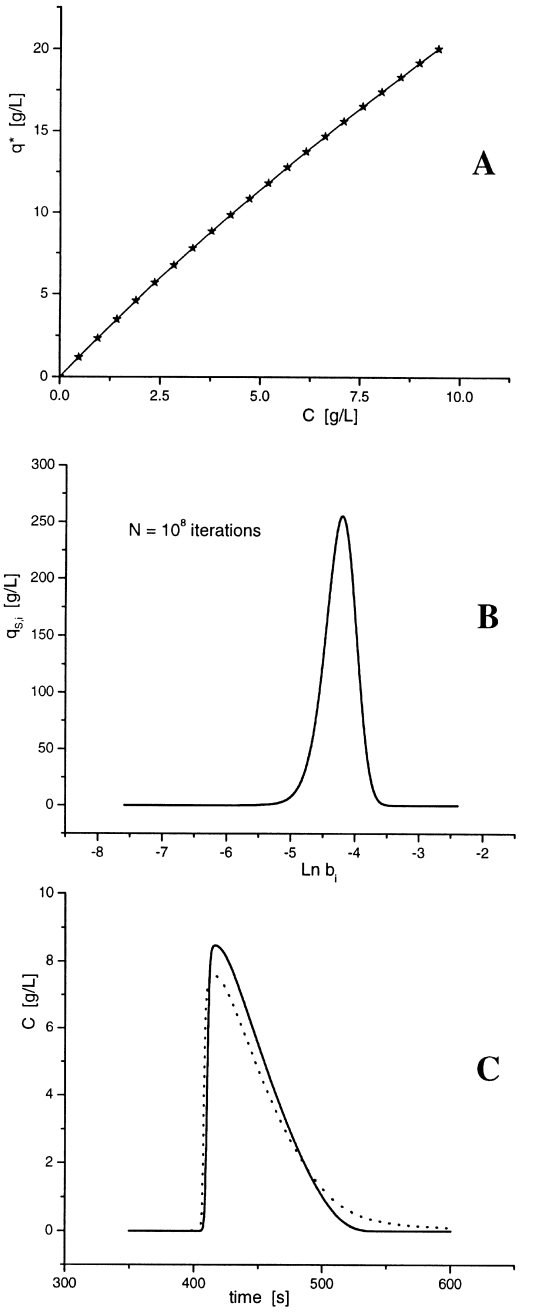

Fig. 6. (A) Experimental isotherm (stars) and best Toth isotherm (solid line) of theophylline on the packed Kromasil-C_{18} column I with methanol–water (30:70, v/v) as the mobile phase. $T = 295$ K. (B) Unimodal adsorption energy distribution calculated from the raw adsorption data by the expectation-maximization method. Local Langmuir isotherm. (C) Comparison between calculated (solid line) and experimental (dashed line) band profile measured on column I.

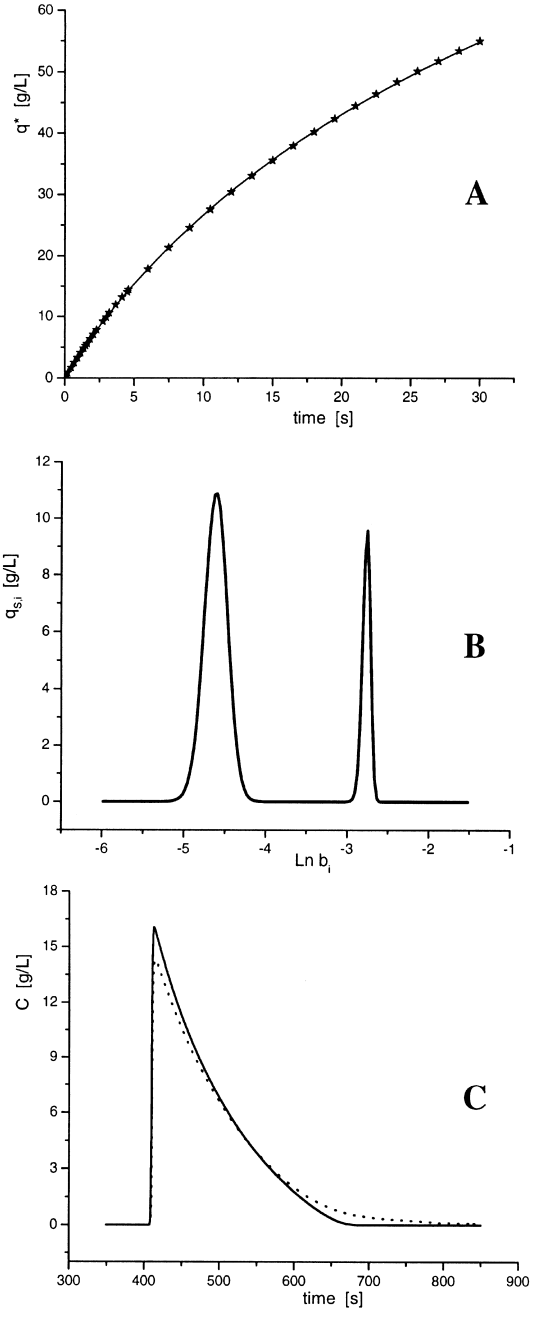

Fig. 7. (A) Experimental isotherm (stars) and best bi-Langmuir isotherm (solid line) of phenol on the packed Kromasil-C_{18} column I with methanol–water (45:55, v/v) as the mobile phase. $T = 295$ K. (B) Bimodal adsorption energy distribution calculated from the raw adsorption data by the expectation-maximization method. Local Langmuir isotherm. (C) Comparison between calculated (solid line) and experimental (dashed line) band profile measured on column I.

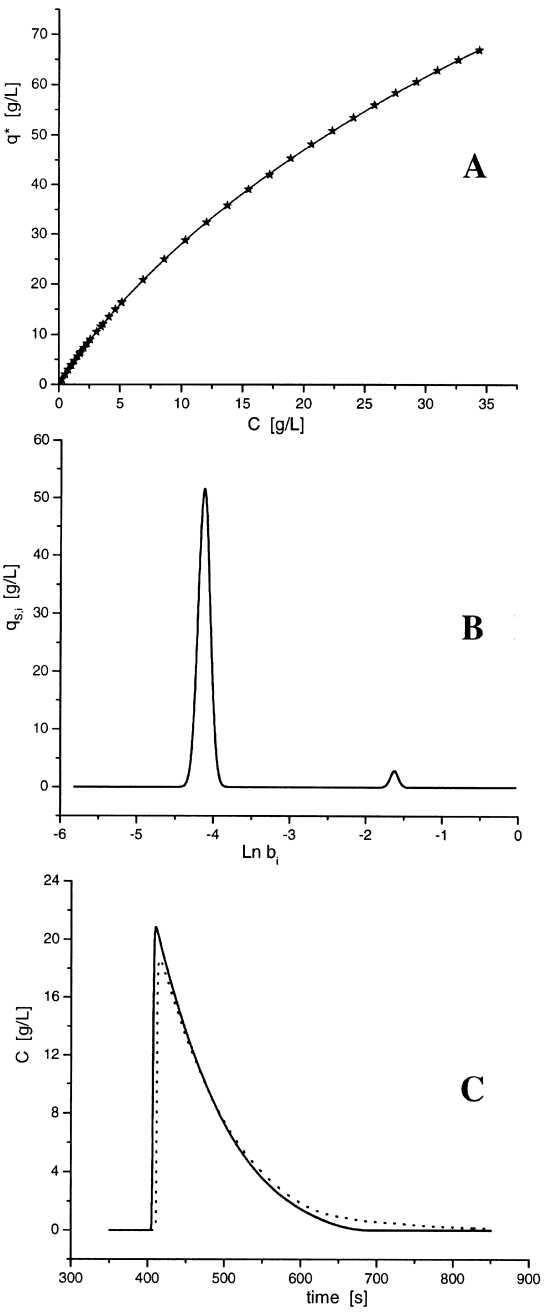

Fig. 8. (A) Experimental isotherm (stars) and best bi-Langmuir isotherm (solid line) of caffeine on the packed Kromasil-C_{18} column I with methanol–water (30:70, v/v) as the mobile phase. $T = 295$ K. (B) Bimodal adsorption energy distribution calculated from the raw adsorption data by the expectation-maximization method. Local Langmuir isotherm. (C) Comparison between calculated (solid line) and experimental (dashed line) band profile measured on column I.

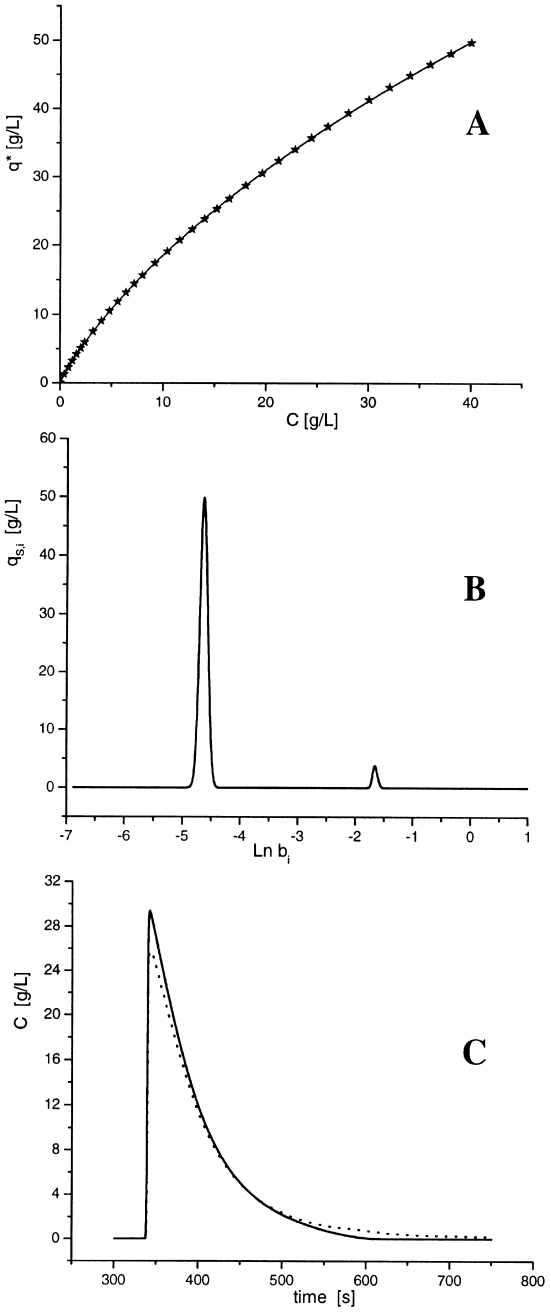

Fig. 9. (A) Experimental isotherm (stars) and best bi-Langmuir isotherm (solid line) of propranolol on the packed Kromasil-C_{18} column I with methanol–water (60:40, v/v) as the mobile phase (acetate buffer at $I = 0.2$ M). $T = 295$ K. (B) Bimodal adsorption energy distribution calculated from the raw adsorption data by the expectation-maximization method. Local Langmuir isotherm. (C) Comparison between calculated (solid line) and experimental (dashed line) band profile measured on column I.

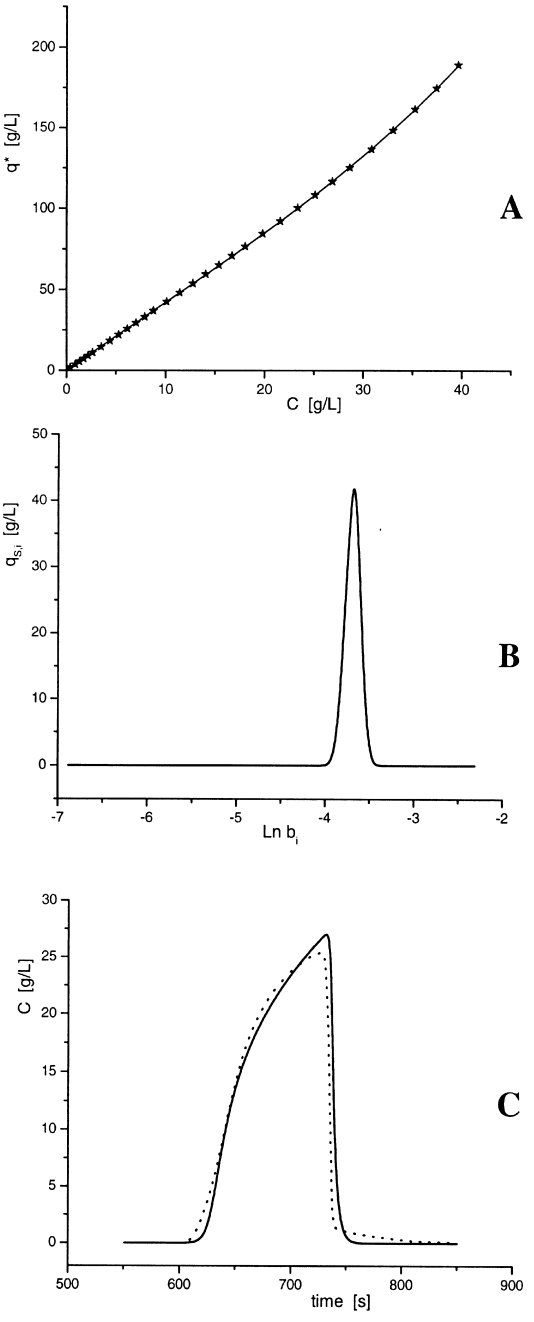

Fig. 10. (A) Experimental isotherm (stars) and best BET isotherm (solid line) of ethylbenzene on the packed Kromasil-C_{18} column I with methanol–water (30:70, v/v) as the mobile phase. $T = 295$ K. Local Langmuir isotherm. (B) Unimodal adsorption energy distribution calculated from the raw adsorption data by the expectation-maximization method. Local BET isotherm. (C) Comparison between calculated (solid line) and experimental (dashed line) band profile measured on column I.

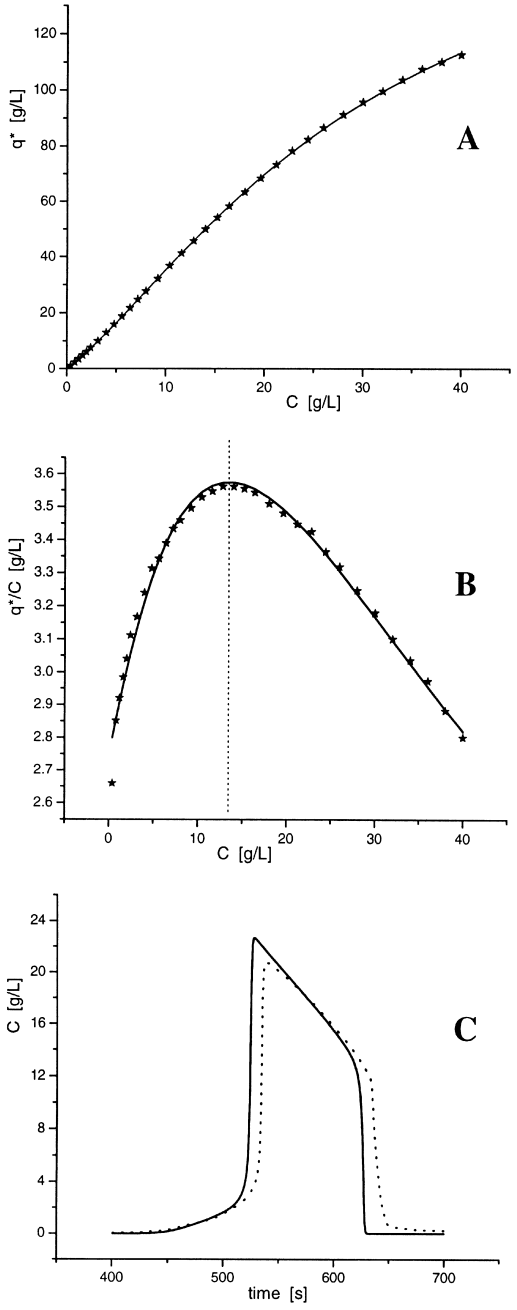

Fig. 11. (A) Experimental isotherm (stars) and best quadratic isotherm (solid line) of propranolol on the packed Kromasil-C_{18} column I with methanol–water (40:60, v/v) as the mobile phase. $T = 295$ K. (B) Experimental isotherm chord q^*/C (stars) and the corresponding quadratic chord (solid line). Note the maximum of the chord at $C \approx 12$–13 g/l. (C) Comparison between calculated (solid line) and experimental (dashed line) band profile measured on column I.

as the Fowler, the Kiselev and the Ruthven models that all assume adsorbate–adsorbate interactions. But the comparison of the calculated and experimental overloaded band profiles led to the dismissal of the former two models. The second order Ruthven model (or quadratic isotherm) accounted well for the isotherm data (Fig. 11A) and for the band profiles (Fig. 11C), with only a slight shift toward higher retention times (+10 s) for the shock layers. The q^*/C plot (Fig. 11B) confirms the position of the rear shock, when the slope of the chord is maximum (for $C \approx 12$–13 g/l).

4.2.6. Comments and conclusion

A few general comments can be made regarding the isotherm parameters derived from the adsorption data measured on column I. Firstly, for all systems studied, which include only low-molecular-mass compounds, the total saturation capacities are systematically between 160 and 190 g/l (the true saturation capacity for the quadratic isotherm is $2q_S$). These results are consistent with the values of the saturation capacities measured on another C_{18} stationary phase (Symmetry from C_{18} from Waters, Milford, MA, USA) with similar low-molecular-mass compounds (3-phenyl-1 propanol, $q_S = 141$ g/l; 4-*tert*.-butylphenol, $q_S = 181$ g/l; and butylbenzoate, around $q_S \approx 150$ g/l) [26]. This relatively narrow range of the saturation capacities suggests that the saturation capacity of a silica-bonded C_{18} stationary phase depends little on the chemical nature of the organic compound involved, but depends mainly on the size of the compound. The fractal structure of the silica surface is likely the cause of this observation. It may explain why Liu et al. [37] measured a saturation capacity of only 20 to 60 g/l for far larger molecules such as insulin ($M_r = 5800$) on another C_{18} silica stationary phase. Obviously, the saturation capacity has an upper limit corresponding approximately to the internal porosity of the packing material. For low-molecular-mass organic compounds this would be of the order of 700 g/l.

Secondly, since the composition of the mobile phase was selected in such a way that the retention factors of all the compounds studied be between 2 and 3 (i.e. their Henry constants were between 3 and

5), it is not surprising that the main adsorption constants be all very close, a few hundreds of l/g.

To summarize, in each specific case the numerical values determined for the various isotherm parameters make physical sense. This confirms the validity of the isotherm models selected.

4.3. Prediction of band profiles from isotherm data measured on column I and comparison with the experimental band profiles measured on nine distinct columns

Figs. 12–18 compare the experimental band profiles recorded for each of the six compounds studied, on each of the 10 columns used, and the corresponding calculated profiles. These profiles were calculated using the isotherm model determined for the packing material from the FA measurements made on column I and the characteristics of the individual column (see Section 3.6.1). The sample size used corresponds to a loading factor of ~10%. The column efficiency was derived in each case following the procedure shown in Fig. 1. It was 2000 theoretical plates for propranolol without buffer in the mobile phase, 2500 plates for aniline, caffeine, phenol, and ethylbenzene and 3200 for theophylline and propranolol in the presence of buffer. These efficiencies were assumed to be the same for all the columns. The rationale for this assumption is that small changes of the column efficiency would not affect much the band profiles at a loading factor of 10% and that a previous study [14] had demonstrated the low RSD for the batch-to-batch reproducibility of the efficiency of the columns used here for the compounds investigated. The experimental profiles in Figs. 12–18 confirm that all the columns have nearly the same efficiency for a given compound, independently of the batch of packing material considered. Thus, the minor variations in the column efficiency have no significant effect on the value of E.

Except for column X, there is an excellent agreement between recorded and calculated profiles in Figs. 12–16, corresponding to the compounds having a Langmuirian isotherm. The differences between the two profiles are more important in Figs. 17 and 18 but remain small, except again in the case of column X. The relative average error E between calculated and recorded profiles (Eq. (21)) is plotted in Fig. 19 for all the chromatographic systems studied. As expected, $|E|$ is lower than 1% for column I. Its average for all columns is very close to 0. This result validates the choice of the peak descriptors as a discrete representation of the band profile. Otherwise, E would have been systematically positive or negative and $|E|$ larger. As expected also since the isotherms were all measured on column I, no other column gives as good an agreement between recorded and calculated profiles (column VII would if it were not for the caffeine data). Out of 70 data points in Fig. 19, only 10 correspond to values of $|E|$ larger than 2.2% and seven of them correspond to the same column, column X (Table 4). This shows an excellent degree of reproducibility of the chromatographic profiles under nonlinear conditions. It is striking that there are no significant differences between the pattern of behavior of the columns coming from the same batch of packing material (column I to V) and that of the columns packed with different batches (columns I, and VI to IX). For all these nine columns the $|E|$ values are below 4% and all but three values are below 2%.

Only column X has a behavior markedly different from that of the other columns. The calculated profiles have always higher retention times than the experimental ones, by up to 10%. There are no obvious explanations. Although column X has a low porosity, so does column IX. It has a low carbon loading but it is similar to that of column VII and higher than that of column VI. This is all the more striking since column X provides values of the retention factors under linear conditions that are similar to those obtained with the other columns (see Fig. 4). Since the band profiles were calculated using the actual total column porosities as measured at the beginning of this study, the only explanation left seems to be that the saturation capacity q_S of column X is significantly lower than those of the nine other columns for as yet an unexplained reason. This cannot be due to a lower value of the adsorption constant b, otherwise the retention factor would be lower and the shape of the band profile, especially the rear diffuse boundary in the case of the compounds with Jovanovic, Toth or bi-Langmuir isotherms, would be steeper. Actually, what we observe in Figs. 12–18 is a mere translation toward lower

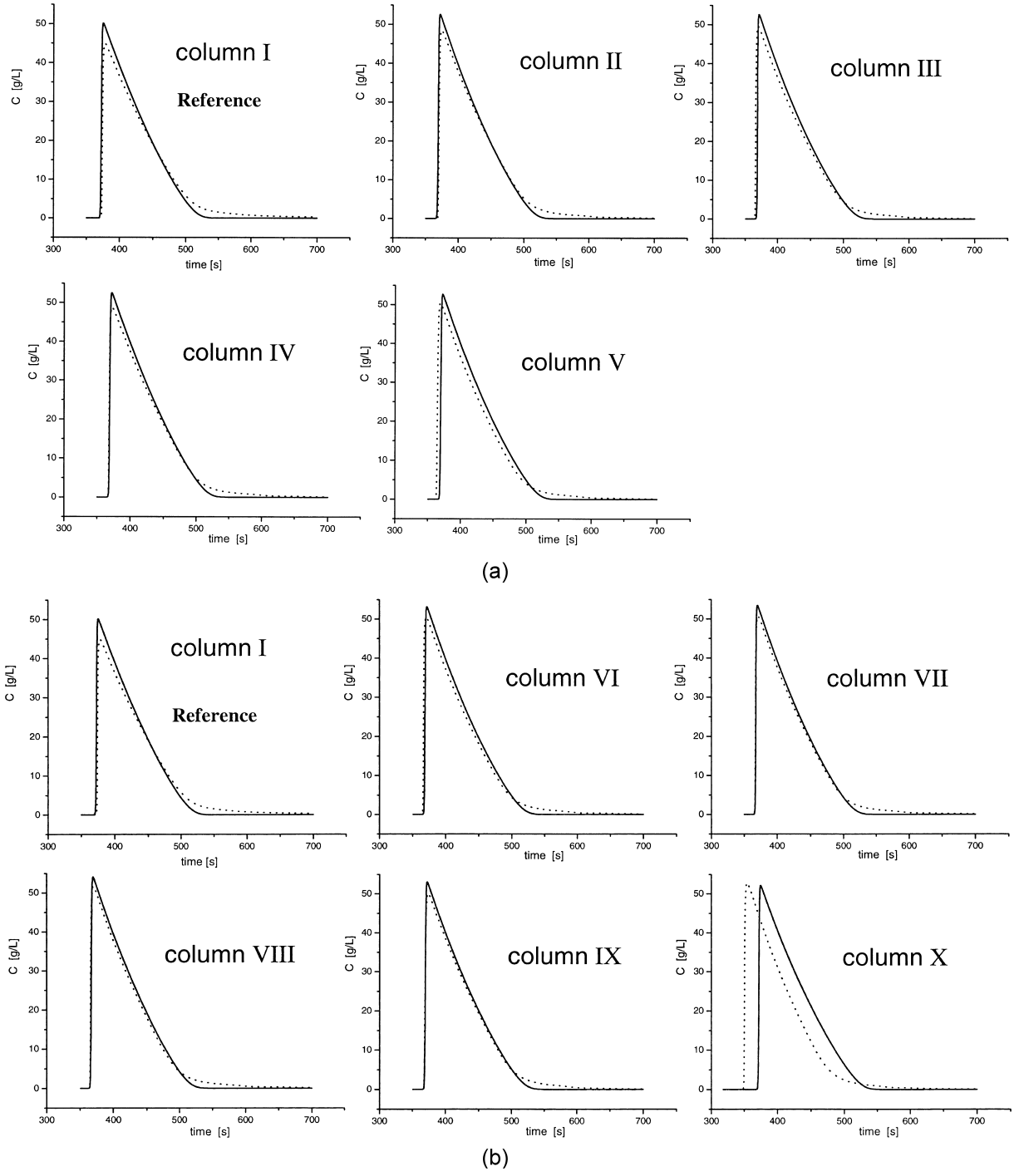

Fig. 12. Comparison between the experimental overloaded (dashed line) and calculated (solid line) profiles of aniline. (A) Column-to-column. (B) Batch-to-batch.

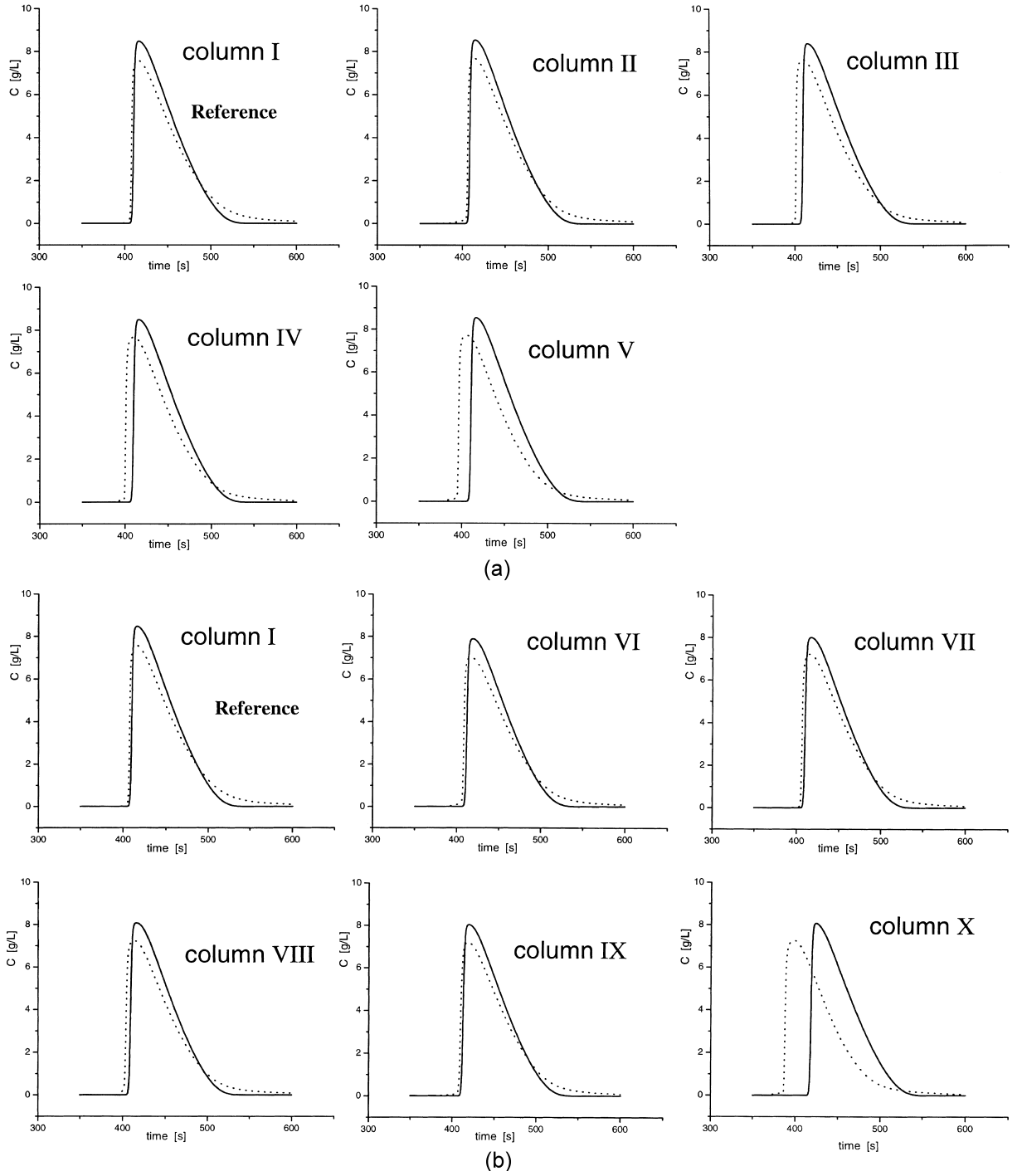

Fig. 13. Comparison between the experimental overloaded (dashed line) and calculated (solid line) profiles of theophylline. (A) Column-to-column. (B) Batch-to-batch.

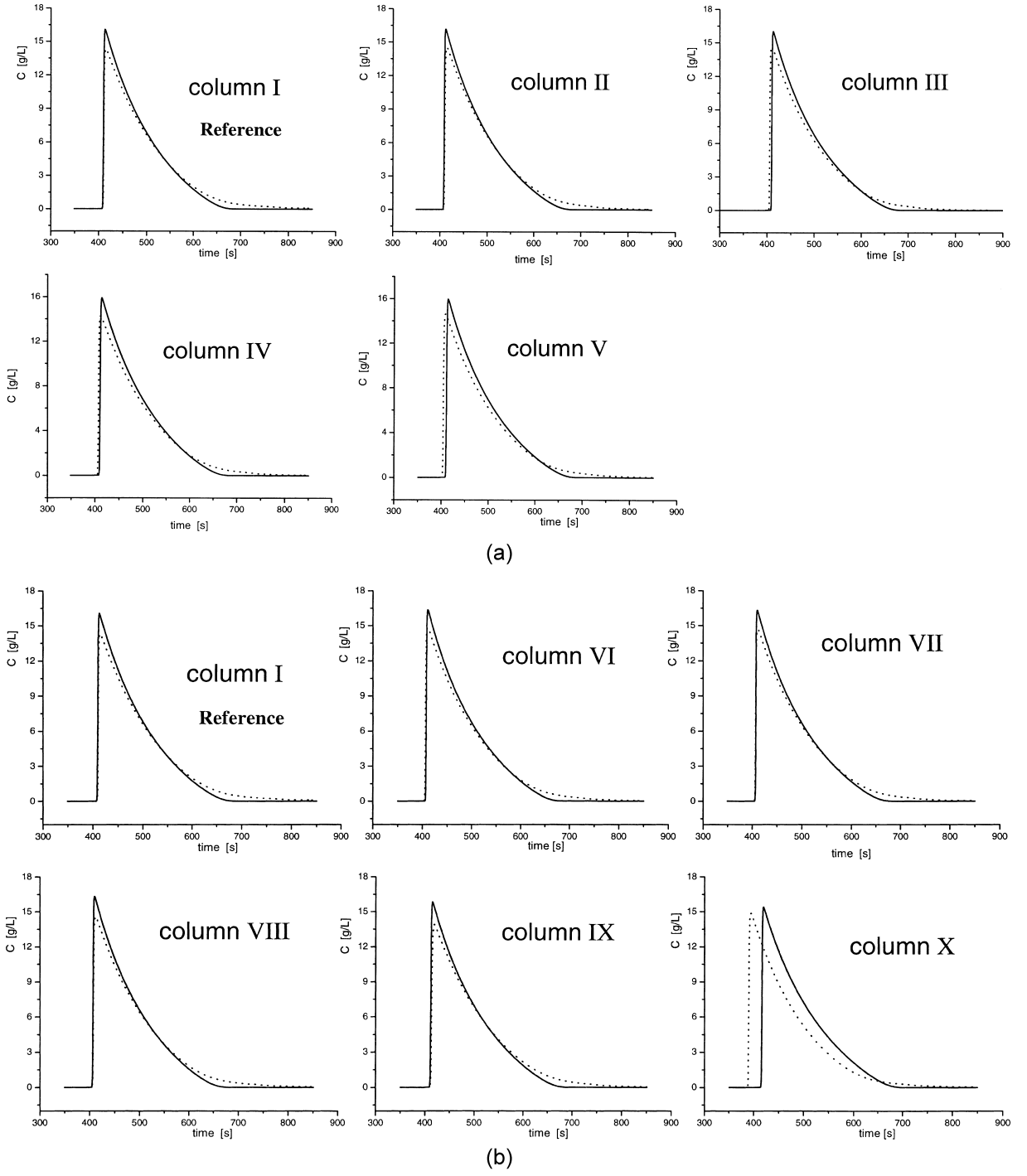

Fig. 14. Comparison between the experimental overloaded (dashed line) and calculated (solid line) profiles of phenol. (A) Column-to-column. (B) Batch-to-batch.

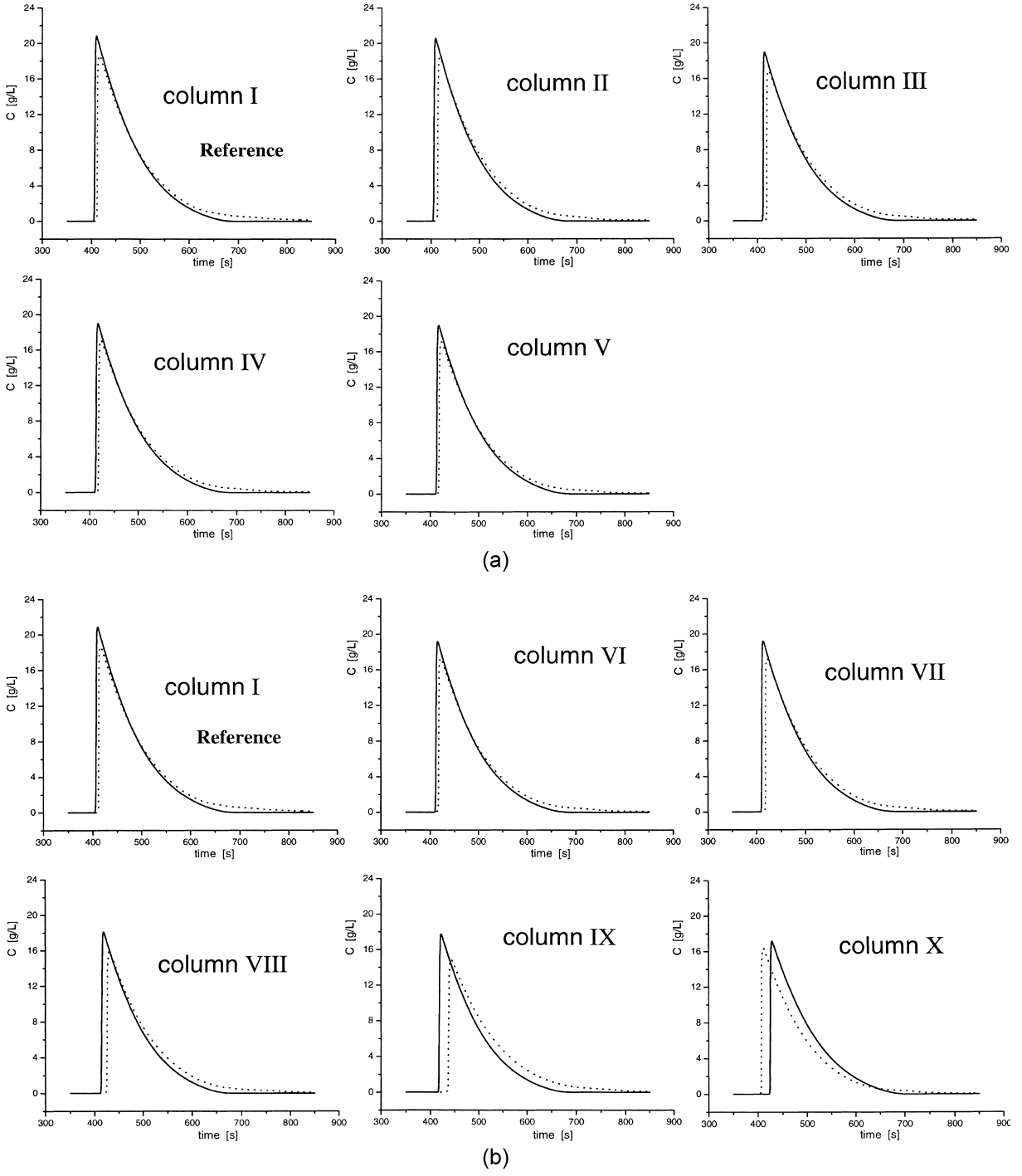

Fig. 15. Comparison between the experimental overloaded (dashed line) and calculated (solid line) profiles of caffeine. (A) Column-to-column. (B) Batch-to-batch.

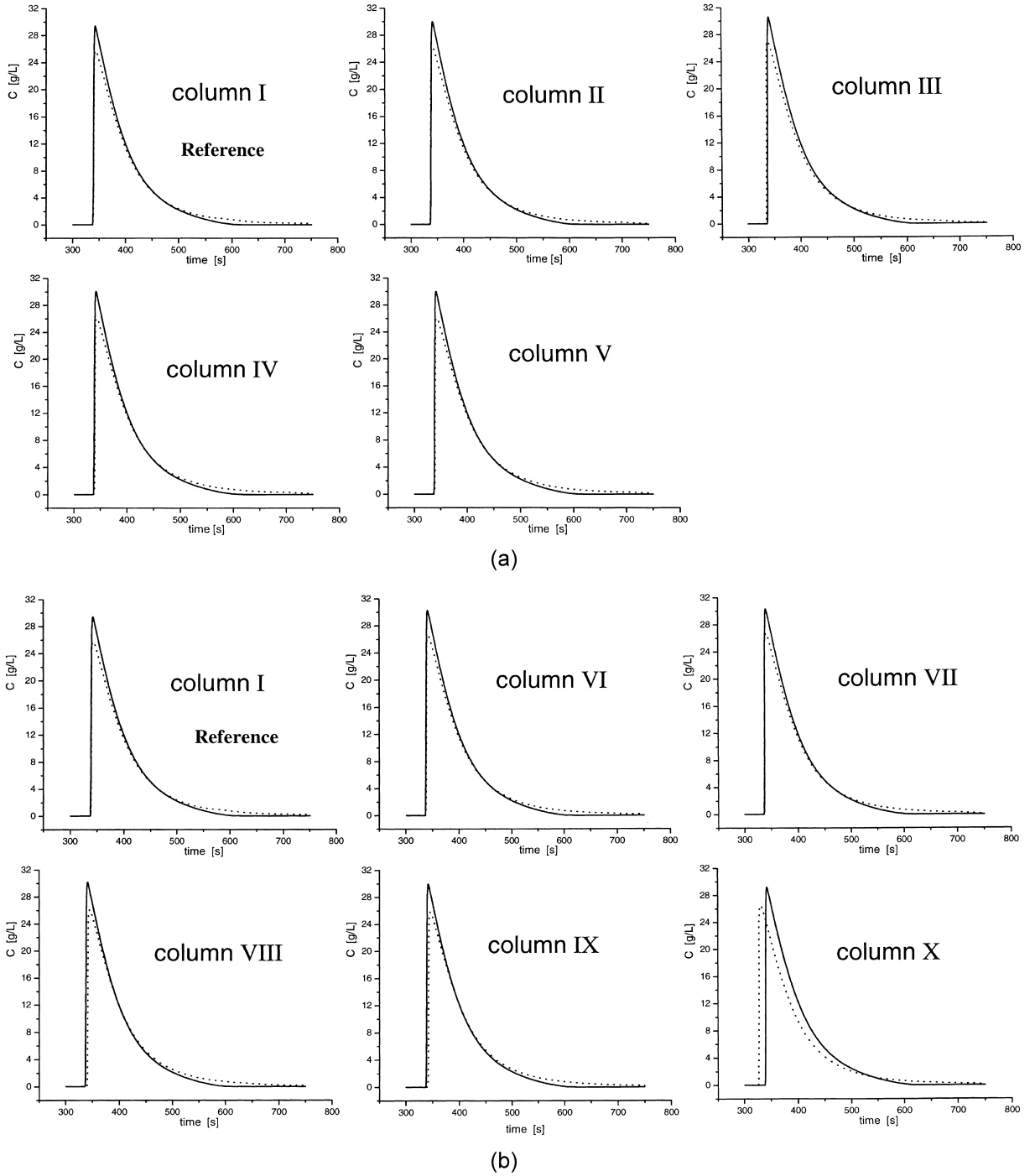

Fig. 16. Comparison between the experimental overloaded (dashed line) and calculated (solid line) profiles of propranolol with acetate buffer in the mobile phase. (A) Column-to-column. (B) Batch-to-batch.

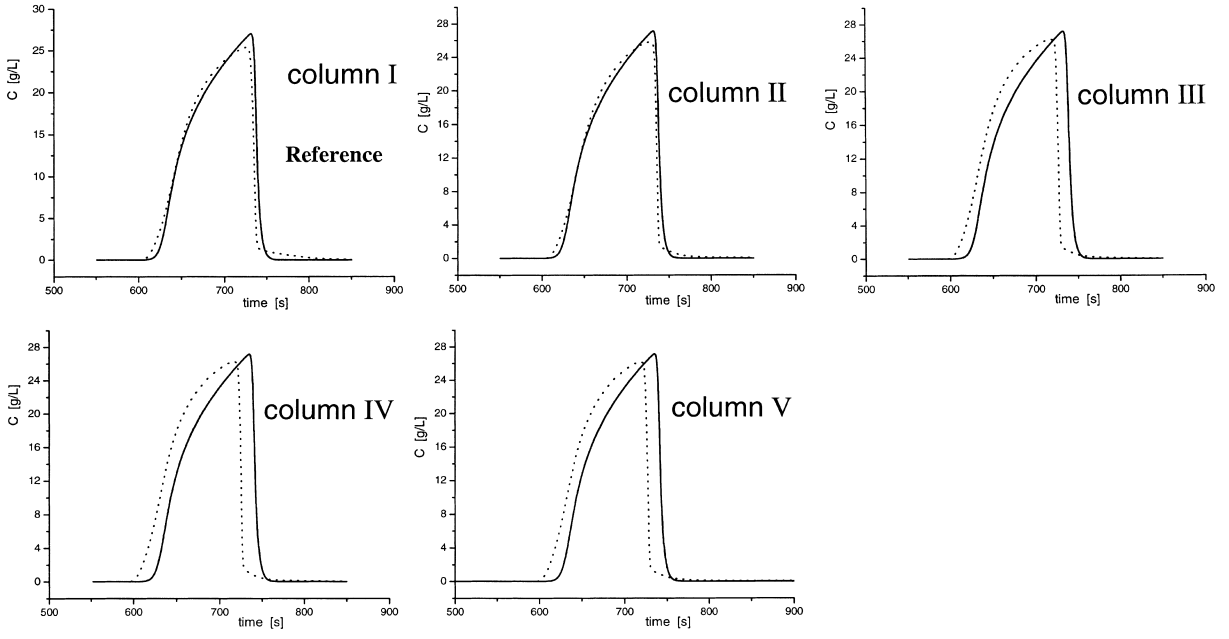

(a)

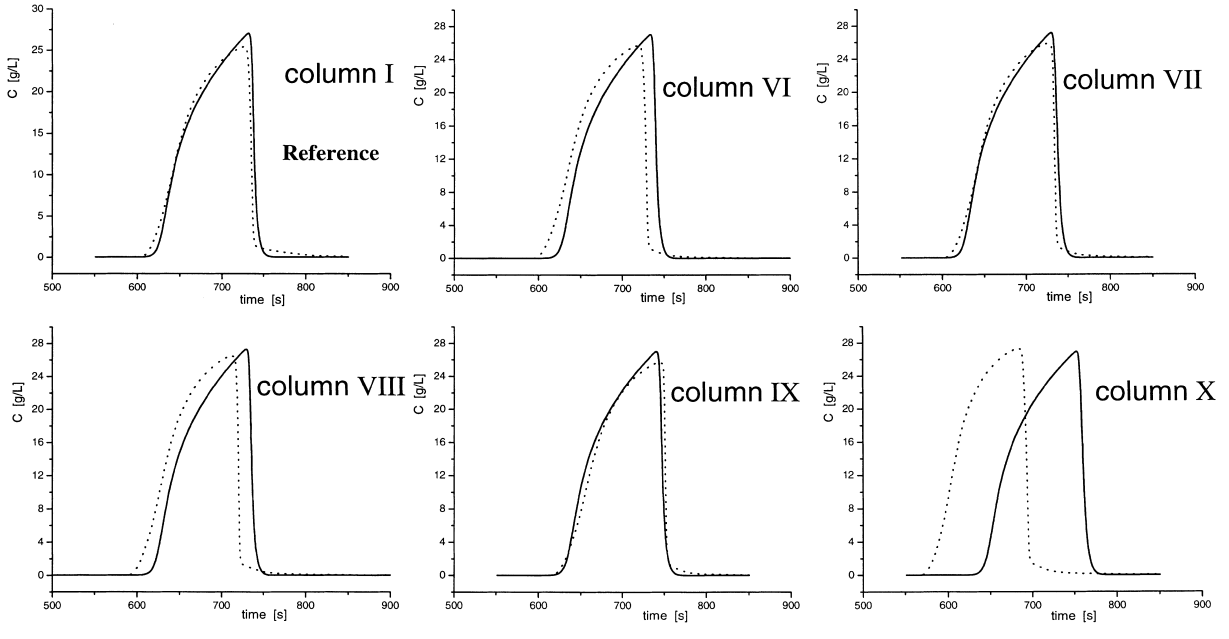

(b)

Fig. 17. Comparison between the experimental overloaded (dashed line) and calculated (solid line) profiles of ethylbenzene. (A) Column-to-column. (B) Batch-to-batch.

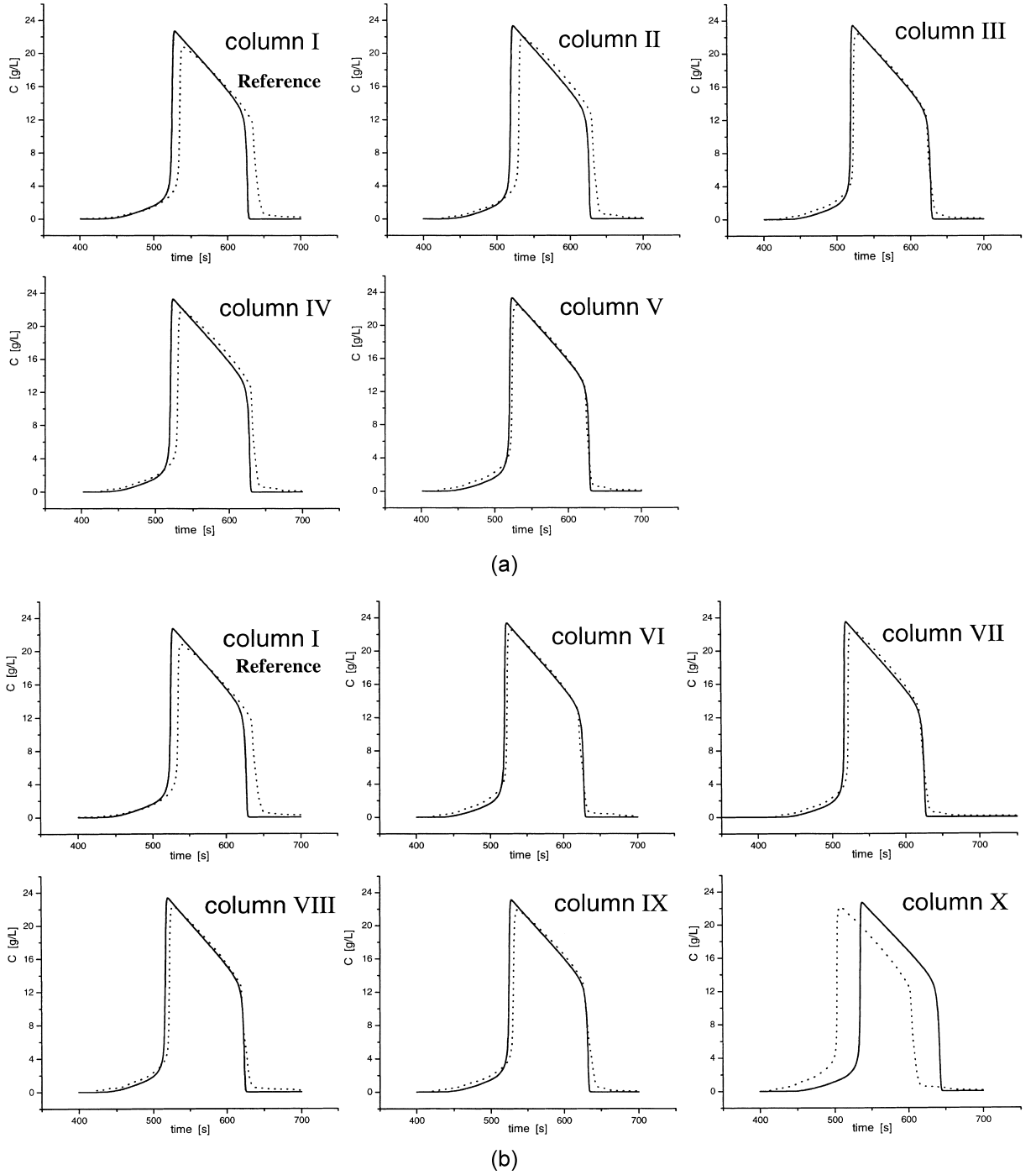

Fig. 18. Comparison between the experimental overloaded profile (dashed line) and the calculated profile (solid line) of propranolol with no buffer in the mobile phase. (A) Column-to-column. (B) Batch-to-batch.

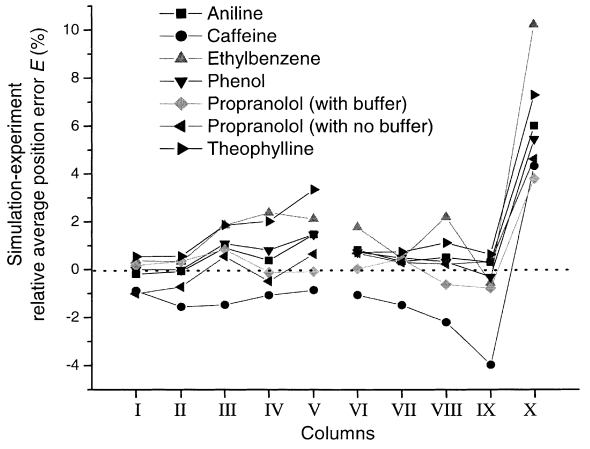

Fig. 19. Relative global error E between calculations and experiments for all the chromatographic systems studied, calculated according to the points defined in Fig. 1. Note the parallel evolution of the curves. Column I to V: same batch. Column I, VI to X: different batches.

retention times of the experimental relative to the calculated band profile.

Another striking result illustrated in Fig. 19 is the parallel evolution of the error E from column to column and from system to system. In other words, for a given column, the list of systems by increasing value of E is the same, with only a few inversions for compounds having always close values of E. For a given system, the variation of E tends to be smooth. This observation is further supported in Table 4 which reports the values of E and also the covariances for each column/column and solute/solute pairs. This covariance is always positive and rather close to 1. The covariance between two columns does not significantly differ whether these two columns belong or not to the same column batch. The covariance between two solutes is quite high, always larger than 0.80. This suggests that the nature of the molecular interactions involved in the retention is very similar for the different columns used. The column to column changes are very minor and do not affect the global relative error in a specific direction. This is consistent with all the measurements having been carried out under reversed-phase conditions, the interactions involved are essentially hydrophobic in nature.

5. Conclusion

Our results demonstrate the excellent reproducibility of the adsorption data measured on 10 Kromasil-C_{18} columns for six different compounds, one of them using two widely different mobile phases. The six compounds studied, aniline, caffeine, ethylbenzene, phenol, propranolol, and theophylline have different physicochemical properties. This results in their isotherm data being best modeled by quite different isotherm equations. The diversity of these models is a first important result of this work: many isotherm models used here are rarely mentioned in the chromatographic literature. This suggests that there might have been and there still may be an excessive emphasis in this literature on the use of the Langmuir model. For any one of these six compounds, however, the band profiles obtained on the 10 columns are extremely similar. With nine out of 10 columns, the differences observed are essentially minor shifts of the elution profiles along the time axis. These shifts are less than 2% in most cases. Even in the case of the one column (X) that seems to differ significantly from the rest of the lot, these shifts never exceeded 10%. For all the chromatographic systems studied, the saturation capacity of this column seems to be significantly lower than that of all the other columns. For the other nine columns, the batch-to-batch reproducibility (five batches) was as good as the column-to-column reproducibility (five columns). Thus, it seems that some modern stationary phases at least have achieved an excellent degree of reproducibility of their chromatographic properties, not only under linear conditions as shown previously [14], but also under nonlinear ones.

The procedure described in this work allows a rapid and economical test of the reproducibility of the adsorption data on a series of columns belonging to the same or to different batches of a given packing material. Only a single, strongly overloaded band profile has to be recorded for each column. If the best isotherm model is needed, e.g. for computer optimization of the experimental conditions of a preparative separation, FA data acquisition needs to be carried out on only one of the columns of the set studied. The best isotherm model for any of the other columns can be adjusted from this first one on the basis of the difference between the retention times of

Table 4
Relative average error E (column, solute) expressed in percentage between the simulated and experimental profiles and the corresponding column–column and solute–solute covariance matrices

	Aniline	Caffeine	Ethyl-benzene	Phenol	Propranolol (buffer)	Propranolol (no buffer)	Theophylline	Column–column covariance									
I	−0.20	−0.89	0.38	−0.01	0.17	−1.01	0.54	**1.00**									
II	−0.08	−1.56	0.33	−0.01	0.35	−0.73	0.56	0.92	**1.00**								
III	0.91	−1.47	1.85	1.09	0.84	0.55	1.86	0.80	0.93	**1.00**							
IV	0.38	−1.07	2.38	0.81	−0.12	−0.49	2.02	0.85	0.79	0.90	**1.00**						
V	1.47	−0.86	2.12	1.47	−0.09	0.65	3.35	0.71	0.73	0.80	0.76	**1.00**					
VI	0.82	−1.06	1.77	0.73	0.04	0.69	0.72	0.54	0.69	0.66	0.73	0.80	**1.00**				
VII	0.34	−1.48	0.47	0.49	0.45	0.29	0.74	0.67	0.90	0.89	0.86	0.98	0.80	**1.00**			
VIII	0.50	−2.20	2.19	0.32	−0.63	0.23	1.11	0.64	0.75	0.54	0.73	0.76	0.98	0.80	**1.00**		
IX	0.30	−3.97	−0.56	−0.31	−0.78	0.32	0.63	0.45	0.73	0.89	0.73	0.77	0.76	0.94	0.76	**1.00**	
X	6.00	4.32	10.21	5.45	3.80	4.61	7.28	0.60	0.50	0.90	0.76	0.80	0.77	0.38	0.84	0.31	**1.00**
Solute–solute covariance	**1.00**	0.88	0.95	0.97	0.88	0.96	0.95										
		1.00	0.93	0.94	0.93	0.80	0.88										
			1.00	0.98	0.88	0.91	0.95										
				1.00	0.92	0.94	0.97										
					1.00	0.84	0.85										
						1.00	0.90										
							1.00										

the high concentration profiles for that column and for the reference one.

Quantitative, more accurate information regarding the column-to-column and batch-to-batch reproducibility of the isotherm parameters between columns can be obtained from one or several high concentration elution band profiles. This requires the use of the numerical method of calculating the isotherms for each column by solving the reversed problem of chromatography and estimating the isotherm parameters from the overloaded profiles, assuming a suitable mathematical form for the isotherm model [12].

Acknowledgements

This work was supported in part by Grant DE-FG05-88-ER-13869 of the US Department of Energy and by the cooperative agreement between the University of Tennessee and the Oak Ridge National Laboratory. We thank Hans Liliedahl and Lars Torstenson (Eka, Bohus, Sweden) for the generous gift of the columns used in this work and for fruitful discussions.

References

[1] G. Guiochon, S. Golshan-Shirazi, A.M. Katti, Fundamentals of Preparative and Nonlinear Chromatography, Academic Press, Boston, MA, 1994.
[2] G. Guiochon, J. Chromatogr. A 965 (2002) 129.
[3] A. Felinger, G. Guiochon, J. Chromatogr. A 796 (1998) 59.
[4] I. Quiñones, J.C. Ford, G. Guiochon, Chem. Eng. Sci. 55 (2000) 909.
[5] D.M. Ruthven, Principles of Adsorption and Adsorption Processes, Wiley, New York, 1984.
[6] G. Schay, G. Szekely, Acta Chem. Hung. 5 (1954) 167.
[7] D.H. James, C.S.G. Phillips, J. Chem. Soc. (1954) 1066.
[8] E. Glueckauf, Trans. Faraday Soc. 51 (1955) 1540.
[9] E. Cremer, G.H. Huber, Angew. Chem. 73 (1961) 461.
[10] F.G. Helfferich, D.L. Peterson, J. Chem. Educ. 41 (1964) 410.
[11] C. Blümel, P. Hugo, A. Seidel-Morgenstern, J. Chromatogr. A 827 (1998) 175.
[12] A. Felinger, A. Cavazzini, G. Guiochon, J. Chromatogr. A 986 (2003) 207.
[13] M. Kele, G. Guiochon, J. Chromatogr. A 830 (1999) 55.
[14] M. Kele, G. Guiochon, J. Chromatogr. A 855 (1999) 423.
[15] M. Kele, G. Guiochon, J. Chromatogr. A 869 (2000) 181.
[16] M. Kele, G. Guiochon, J. Chromatogr. A 913 (2001) 89.
[17] M. Kele, G. Guiochon, J. Chromatogr. A 960 (2002) 19.
[18] G. Zhong, P. Sajonz, G. Guiochon, Ind. Eng. Chem. (Res.) 36 (1997) 506.
[19] M. Jaroniec, R. Madey, Physical Adsorption on Heterogeneous Solids, Elsevier, Amsterdam, 1988.
[20] R.J. Umpleby II, S.C. Baxter, Y. Chen, R.N. Shah, K.D. Shimizu, Anal. Chem. 73 (2001) 4584.
[21] D.S. Jovanovic, Colloid Polym. Sci. 235 (1969) 1203.
[22] D. Graham, J. Phys. Chem. 57 (1953) 665.
[23] J. Toth, Acta Chem. Hung. 32 (1962) 31.
[24] J. Toth, Acta Chem. Hung. 69 (1971) 311.
[25] S. Brunauer, P.H. Emmet, E. Teller, J. Am. Chem. Soc. 60 (1938) 309.
[26] F. Gritti, W. Piatkowski, G. Guiochon, J. Chromatogr. A 978 (2002) 81.
[27] B.J. Stanley, S.E. Bialkowski, D.B. Marshall, Anal. Chem. 65 (1993) 259.
[28] J. Toth, Adsorption, Marcel Dekker, New York, 2002.
[29] B.J. Stanley, G. Guiochon, J. Phys. Chem. 97 (1993) 8098.
[30] M. Suzuki, Adsorption Engineering, Elsevier, Amsterdam, 1990.
[31] P.W. Danckwerts, Chem. Eng. Sci. 2 (1953) 1.
[32] P. Rouchon, P. Valentin, M. Schonauer, C. Vidal-Madjar, G. Guiochon, J. Phys. Chem. 88 (1985) 2709.
[33] P. Rouchon, M. Schonauer, P. Valentin, G. Guiochon, Sep. Sci. Technol. 22 (1987) 1793.
[34] G. Guiochon, S. Golshan-Shirazi, A. Jaulmes, Anal. Chem. 60 (1988) 1856.
[35] F. Gritti, G. Götmar, B.J. Stanley, G. Guiochon, J. Chromatogr. A 983 (2003) 51.
[36] F. Gritti, G. Guiochon, J. Colloid Interface Sci., in press.
[37] X. Liu, P. Szabelski, D. Zhou, G. Guiochon, J. Chromatogr. A 988 (2003) 205.